Submitted on 24 Aug 2015

Anonymous Referee #1

The authors have given satisfactory answers and corrections to most of my specific comments. However, there are several comments where my remarks were partially neglected or misunderstood; I have listed these below along with my comments. Moreover, the authors have given no reply whatsoever to my general comments. Both of these issues need to be addressed for the paper to be publishable.

Author's answer: We are sorry not to mention about general comments in the previous review. First, we would like to answer to the previous general comments.

Author's answer of general comments in the previous review:

1). A clear shortcoming of the paper is the treatment of the radar parameters, which seem to have been added to the paper as something of an afterthought. There are two glaring omissions: First, as far as I can see, the authors do not mention anywhere in the paper what frequency is assumed for the radar calculations. While the definition of reflectivity in Eq. (11) is frequency independent, the other radar parameters such as Z_dr and K_dp certainly are not! Second, neither the abstract nor the title mention that the paper reports any radar-related analysis.

Author's answer: Thank you for your comment. The polarimetric radar variables are calculated by the scattering simulation (T-matrix simulation) using observed DSD data. We added radar frequency and the other parameters required for T-matrix in the manuscript as follows;

[Page 11, Line 215-218]

"The T-matrix method used in this study is initially proposed by Waterman (1965, 1971) to calculate electromagnetic scattering by single non-spherical raindrops. The adaptable parameters for this calculation are frequency, temperature, hydrometeor types, raindrop's canting angle and drop axis ratio and explained the following sentences."

And we have already added the following sentence in abstract.

[Page 2, Line 23-26]

"Also, to find the dominant characteristics of polarized radar parameters which is differential radar reflectivity (Z_{dr}), specific differential phase (K_{dp}) and specific attenuation (A_h), T-matrix scattering simulation was applied in present study.."

2). The choice of Jarvenpaa as a comparison to Busan also seems a bit arbitrary. Why compare the Busan results to that place in particular? The authors have cited several other papers dealing with DSDs in different regions. As the typical rain intensities and dominant cloud types around the world are highly variable, there will surely be differences between the DSDs as well. As a minimum, I'd suggest adding, if possible, to Table 2 the mean values from the Darwin measurements that the authors have already

referenced. With Darwin near the equator, Busan around 35 deg latitude, and Jarvenpaa around 60 deg, these three would already give a decent comparison in terms of latitude coverage.

Author's answer: Thank you for your comment. As your comment, we would like to know the differences of DSD feature between just two different latitude regions, because there are many researches on the characteristics of DSD in the equator. Anyway, we already removed the sentence and Table 2 according to the recommendation of editor.

3). I found the reported results on the differences between the daytime and nighttime DSDs interesting. A nice way to improve the paper would be to put a bit more effort on this analysis. Specifically, the daytime and nighttime should be separated by the actual sunset and sunrise times (see my specific comments above). The authors speculate that the day-night difference is due to a change in the prevailing winds (continental vs. maritime). This hypothesis could also be tested by separating the observations according the actual measured wind direction. The authors already have this data from the local AWS station so doing this analysis should not be overly difficult.

Author's answer: Thank you for your comment. We used actual sunrise and sunset time provided by Korea Astronomy and Space Science Institute (KASI) as mentioned in the chapter of 2.4, even we took the latest sunrise and earliest sunset time for each classified group (the entire period, summer and winter season) as representatives. Because the present study is focused on the statistical analysis, we would like to choose the time for day and night as representatives.

And we have added Figure 8g and Figure 11d to explain the characteristics of DSDs with variation of wind as Referee's comment. We also described the features in the manuscript as follows;

[Page 19-20, Line 409-413 for Figure 8g]

'~. These variations considerably matched with the diurnal sea wind time series (Fig. 8g). Sea wind is considered as the sum value of normalized wind frequency between 45° and 225°. From 0200 (1400) KST to 1200 (2000) KST shows smaller (larger) value of sea wind frequency which is opposite to the relatively larger (smaller) parts of each parameter (D_m, R, LWC and Z).'

[Page 23, Line 480-483 for Figure 11d]

'~ Alike to the D_m and $log_{10}(N_w)$, normalized frequency of sea wind for Winter season shows inverse relationship to that of Summer season (Fig. 11d). The value of frequency generally decreases (increases) from 0400 (1400) KST to 1400 (0400) KST. Also, it shows symmetry pattern with that of Summer season.'

How were snow events detected? How about hail or graupel?

Author's answer: Thank you for Referee's comment. The present study is focused on liquid raindrops. Therefore, we did not consider the snow, hail and graupel.

My point with this question was: how did you identify events with snow, hail or graupel, so that they were not included in the rain statistics? This is important precisely because this is a liquid raindrop study.
Author's answer: Thank you for your comment and I am sorry to make Referee misunderstand. We do not have an algorithm to classify hydrometeor types automatically. Therefore, we used the surface weather map and surface observational data by KMA (Korea Meteorological Administrator). Furthermore, snowfall and hail are very rarely observed in the research area, southern part of Korea.
[There is no add or modify]

Lines 14-16: The sentence after (ii) is unclear. I don't understand what "DSD spectra was smaller than five consecutive channels" means.
Author's answer: I am so sorry to make you confused. It means that the raindrop should be recorded at more than five channels for one minute (e.g., DSD spectra observed at 1st 2nd, 3rd, 4th and 5th (consecutive) channel of POSS is used, but those of 1st, 2nd, 4th, 5th and 6th (not consecutive) is removed as noise.

The explanation in the comment makes sense, however point (ii) is still unclear in the revised manuscript. I suggest rewording it as follows: "ii) DSD spectra in which drops were not found in at least five consecutive channels were removed as non-atmospheric."
Author's answer: Thank you for your comment and I am sorry that you did not satisfy my previous answer. We sufficiently understood Referee's proposed sentence. So we modified the sentence according to Referee's recommendation.

[Page 23-24, Line 187-188]
"ii) DSD spectra in which drops were not found in at least five consecutive channels were removed as non-atmospheric."

Line 19: How common were cases with R > 200 mm/h?
Author's answer: I'm really so sorry, I do not understand this question exactly. For my understanding, when rain rate (R) exceed 200 mm h-1, disdrometer has a tendency to reduce of detection capacity of small raindrops. Therefore, we removed the samples in case of R > 200 mm h-1 to eliminate the noisy data.

My point was: how often did you get DSD spectra with R > 200 mm/h? I asked this because heavy rainfall cases contribute a significant fraction of the total rainfall, and so ignoring them might lead to some statistical bias.
Author's answer: Thank you for your kindness. There is a table which shows total number (67) of rain rate larger than 200 mm h^{-1}. This is occupied about 0.067% of the entire data (99,388).

Table 1. The total number and value of rain rate in the POSS data larger than 200 mm h^{-1}.

Num.	Rainrate (mm h^{-1})	Num.	Rainrate (mm h^{-1})	Num.	Rainrate (mm h^{-1})	Num.	Rainrate (mm h^{-1})	Num.	Rainrate (mm h^{-1})	Num.	Rainrate (mm h^{-1})	Num.	Rainrate (mm h^{-1})
1	3720.9	11	304.9	21	256.3	31	210	41	253.7	51	292.5	61	229.8
2	274.5	12	228.9	22	385.4	32	233.2	42	256.4	52	261.7	62	309.9
3	4083.7	13	373.2	23	362.4	33	224.7	43	201.6	53	261.7	63	357.9
4	761.7	14	226.1	24	767.8	34	864.3	44	233.8	54	206.9	64	374
5	870.2	15	640.4	25	1194	35	372.2	45	387.2	55	1935.4	65	279.3
6	261.8	16	351.5	26	330.2	36	203.9	46	1308.3	56	237.4	66	233.9
7	225.5	17	331.2	27	1120.4	37	212.7	47	814.8	57	388.1	67	200.4
8	346.3	18	218.6	28	314.2	38	256.8	48	1722.2	58	222.7	·	·
9	795.2	19	230.7	29	210.3	39	435.5	49	244.3	59	405.8	·	·
10	1052.6	20	336.4	30	1074.2	40	541.6	50	634.5	60	212.9	·	·

Line 21: The threshold below which the DSD is overestimated depends on the disdrometer. Leinonen et al. (2012) used a different type of disdrometer.

Author's answer: Thank you for Referee's opinion. I agree to Referee's idea. As far as I know, the tendency of overestimating DSD in $D_0 < 0.5$ mm would be caused by characteristics of disdrometer type. However, it is also by intrinsic feature and threshold of gamma DSD model (Bringi et al., 2003; Leinonen et al., 2012). Therefore, I think it is possible to use this threshold in the present study.

I cannot find an indication that this is an intrinsic feature of the Gamma DSD in either the Leinonen or Bringi papers. Considering that the Gamma DSD is used all the way down to cloud droplet sizes (on the order of 0.01 mm, see e.g. Miles et al. (2000), J. Atmos. Sci., 57, 295–311.), I find this a dubious statement.

Author's answer: Thank you for your comment. We cited the reference sentences as follows;

Bringi et al., (2003) :

<363 page, Appendix A from 1st line to Eq. (A1)>

Radar Retrieval of DSD Parameters:

The method of retrieving D_0, N_w, and μ from Z_h, Z_{dr} , and K_{dp} is summarized here from Gorgucci et al. (2001, 2002). A gamma DSD model is assumed with the following ranges for the parameters:

$0.5 < D_0 < 3.5$ mm (A1)

Leinonen et al., (2012) :

<395 page, 2.Data filtering(e), from 3rd line to last.>

In addition, simulations of DSD truncation in gamma distributions showed that Eq. (4) overestimates D0 at low values. The error decreases rapidly as the true D_0 increases, being less than 20% for $D_0 > 0.5$ mm if $\mu = 0$; for higher values of m, the decrease is even faster. Thus, only distributions for which $D_0 > 0.5$ mm were considered to be acceptable for inclusion in the statistics; these were included without further modification.

Finally, the present study only consider the raindrop not cloud droplet.

Line 3: What T-matrix implementation was used? Eq. (11): This equation holds for the Rayleigh scattering regime; since you have omitted the radar wavelength, I cannot evaluate if it is applicable to Referee's calculations.
Author's answer: I'm so sorry, I missed that. The radar frequency in the T-matrix simulation is considered as S-band (2.85 GHz). I added the specification of this in the present study 'Also, the condition of frequency for electromagnetic wave of radar is 2.85 GHz (S-band).'

The question about which T-matrix implementation was used in this study has not been answered.
Author's answer: Thank you for your comment and we feel sorry to misunderstand Referee's meaning. First of all, radar reflectivity facto (z) and horizontal polarized radar reflectivity (Z) is not related to T-matrix but is calculated from DSD collected by POSS directly. Therefore, we moved the sentence to the next of Equation 13 to avoid confusing and we modified the sentence as follows;

[Page 11, Line 215-218]
'The T-matrix method used in this study is initially proposed by Waterman (1965, 1971) to calculate electromagnetic scattering by single non-spherical raindrops. The adaptable parameters for this calculation are frequency, temperature, hydrometeor types, raindrop's canting angle and drop axis ratio and explained the following sentences.'

[Page 31, Line 676-677]
'Waterman, P.C.: Matrix formulation of electromagnetic scattering. Proc. IEEE, 53, 805-812, 1965.'

Also, the more detailed information for T-matrix will be found on the web page:
http://www.giss.nasa.gov/staff/mmishchenko/t_matrix.html.

References
Waterman, P.C.: Matrix formulation of electromagnetic scattering. Proc. IEEE, 53, 805-812, 1965.

Waterman, P.C.: Symmetry, unitarity, and geometry in electromagnetic scattering, Physical review D, 3, 825, 1971.

Submitted on 09 Sep 2015

Anonymous Referee #4

The paper was improved even if I regret that it contains too many descriptions of the figures but not enough associated physical interpretations. New elements that the authors have been added (the POSS description in particular) are sometime a bit confusing. Moreover, I have found some other mistakes in the manuscript. I am sorry that a part of my new comments was not in my first review but I think it is important to take them into account. The last figures have been also modified and I think that some errors have appeared… I'm afraid that this paper is not totally ready for publication.

• Page 8, line 145: I am surprised by the value of water density assumed by the authors. I think that 1 g m-3 should be changed into 10^6 g m-3, isn't it?

Author's answer: Thank you for your comment and I am sorry type error makes you confusing. Originally, I would like to explain as 1 g cm^{-3}. Of course, there is no problem to the results and we modified as 1×10^{6} g m^{-3} in the manuscript.

[Page 8, Line 146]

'~ it assumed as 1×10^{6} g m^{-3}'

• Page 8, line 150: "Unis" should be changed into "Unit".

Author's answer: Thank you for your comment. I modified as your opinion.

[Page 8, Line 152]

'~ mass flux unit (mg m^{-2} s^{-1})'

• Page 8, line 150-151: This factor just corresponds to the conversion of length units into mm and time units into hours.

Author's answer: Thank you for your comment. Rainrate (R) would be considered as a mass flux moving from atmosphere to the ground. The unit of flux for some physical quantity (X) is X m^{-2} s^{-1}. For example, the unit of heat flux is considered as J m^{-2} s^{-1}. Therefore, rainfall would be considered as a mass flux (mg m^{-2} s^{-1}). To match with the standard unit of rain rate (mm h^{-1}), 3.6×10^{-3} needs to change the unit from mass flux (mg m^{-2} s^{-1}) to rain rate (mm h^{-1}). Also, $\pi/6$ changes the shape of raindrop from cube to sphere to calculate accumulated height (mm) of rainwater correctly.

[There is no add or modify]

• Page 8, line 161, last sentence: "Using DSD estimate" is confusing because it mixes the principle of the POSS radar for DSD estimation (I understood that POSS radar estimate DSD from Doppler spectra) and the POSS calibration technique.
Indeed Johnson and Hamilton (2008) explained in their section 4 that N(D) was estimated by inverting their equation (2) (corresponding to your equation (11)) using predetermined weighting functions. They explained also in their section 3 that "The "forward" equation (2) could also be used to calculate S(f) for hypothetical N(D)".
Author's answer: Thank you for your detail explanation. I modified as

[Page 8, Line 162]
'To estimate DSD, Doppler power density spectrum ~'

• Same part: X (in V(X)) is not defined.
Author's answer: Thank you for your comment. The symbol 'x' means arbitrary parameters which affect the sampling volume V(x). We added the definition in the manuscript as follows;

[Page 9, Line 171]
'~ and the symbol 'x' means arbitrary parameters which affect the sampling volume**'**

• Page 9, line 170 : I propose to change « A Doppler » by « The Doppler »
Author's answer: Thank you for your comment and I modified it as Referee's opinion.

[Page 9, Line 172]
'The Doppler ~'

• Page 9, line 185, I don't understand the meaning of the sentence: "Number of DSD was smaller than …" It means that the authors compare between the number of spectra with a number of channels (I understood that it corresponded to velocity or diameter classes) ? What do you think about this proposition: "Non-atmospheric data were removed from the analysis if the DSD spectrum was concentrated in less than five consecutive channels,…"
Author's answer: Thank you for your comment. I am sorry that corrected sentence makes you confusing again. We are completely understand for Referee's suggested sentence. However, First Referee already suggested as 'ii) DSD spectra in which drops were not found in at least five consecutive channels were removed as non-atmospheric.' So we would like to ask you to modify the sentence as First Referee's recommend carefully. Thank you for your considerations.

[Page 23-24, Line 187-188]
"ii) DSD spectra in which drops were not found in at least five consecutive channels were removed as non-atmospheric."

• Figure 3: PSN C-band radar is plotted but it is not used and not described in the text. I propose to delete it.

Author's answer: Thank you for your comment. I removed the signature with respect to the PSN C-band radar in Figure 2.

[Page 32, Figure 2]

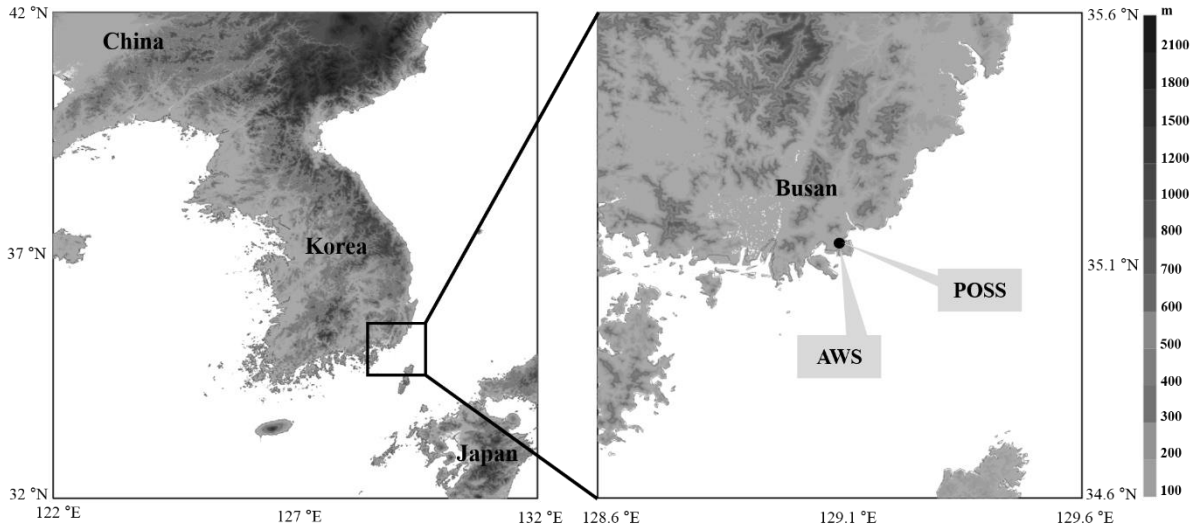

Figure 2.

Locations of the POSS and the AWS rain gauge installed in Busan, Korea.

• Page 12, line 236-237: The authors introduced classification methods for rainfall type via the analysis of 3 microphysical characteristics. For the first one, they mentioned a N0-R relationship. But they did not explain how N0 or/and R is/are used to classify as stratiform or convective rain.

Author's answer: Thank you for your comment. It is simple example of the classification of rainfall type using DSD parameter. To avoid confusing, we will modify the explanation as follows;

[Page 12, Line 244-245]

'R ($N_0 > 4 \times 10^9 R^{4.3}$ in $m^{-3}mm^{-1}$ is considered as convective rainfall, Tokay and Short, 1996; Testud et al., 2001)'

• Page 12, line 240: R<0.5 mm h-1 during 5 minutes is equivalent to 0.04 mm during 5 minutes. I thought it was very low threshold for convective rainfall! So, I checked in Johnson and Hamilton (1988) and I found that they mentioned that the threshold is 0.5 mm per 5 min (that corresponds to 6 mm h-1). The sentence should be therefore modified in the manuscript. Hopefully, the classification method proposed by Bringi et al. (2003) is applied in the present study.

Author's answer: Thank you for your advice. Referee's comment is absolutely right. So we modified as follows;

[Page 12, Line 248-249]

'~ value larger than 0.5 mm per 5 min is considered as convective rainfall (Johnson and Hamilton, 1988)'

• Page 14, line 279: I think that "0<μ>5" should be replaced by "0<μ<5"

Author's answer: Thank you for your comment. We modified the expression as Referee's comment.

[Page 14, Line 289]

'0<μ<5'

• Figure 4, a bracket is missing in the caption just after " solid blue line"

Author's answer: Thank you for your comment. We added the close bracket.

[Page 41, Figure 4]

'PDF and CDF curves for (a) μ, (b) D_m, (c) $\log_{10}(N_w)$, (d) $\log_{10}(R)$, (e) $\log_{10}(LWC)$, (f) Z, (g) Z_{dr}, (h) K_{dp}, and (i) A_h for the entire rainfall dataset (solid black line), stratiform rainfall (solid green line), and convective rainfall (solid blue line). The solid red line represents the CDF for entire rainfall dataset. The solid vertical line represents the mean value of each type**'**

• Page 20, line 417: the double bracket should be transformed into a simple one

Author's answer: Thank you for your comment. We removed a duplicated expression.

[Page 20, Line 430]

'$\log_{10}$(LWC)'

• Section 3.1. and 3.3.1.: I regret that there is too much figures description and not enough associated physical interpretations.

Author's answer: Thank you for your opinion. Of course it is one of the important results for the present study but it is not core contents. Our purpose is to show the general distribution of DSD and radar parameters which are collected during long-term period.

[There is no add or modify]

• Figure 12 and 13: I think that "NT" and "DT" should be replaced by "Winter" and "Summer" in the legends as well as in the captions. I am confused also because your previous figure 14(b) in the first version of the manuscript is the same as the figure 12(c) in the new version of the manuscript whereas the captions are different.

Author's answer: Thank you for your comment and I am sorry it makes you confusing. We missed the explanation about the considered rainfall type. Figure 12 is PDF and CDF of daytime (DT) and nighttime (NT) for the entire rainfall type in summer and winter season, respectively. Also, Figure 13 is same as Figure 12 but for convective rainfall type in summer and winter season, respectively. We added the considered rainfall type in Figure 12 to avoid confusing.

[Figure 12, Page 50, Line 861]

'PDF and CDF of (a) D_m ((b) D_m) and (c) N_w ((d) N_w) for the entire rainfall type in the Summer (Winter) season. ~'

Also, the caption of Figure 9 was modified to avoid confusing as;

[Figure 9, Page 47, Line 831]

'~ for DT and NT according to the entire period. The solid ~'

,

The caption of Figure 14 in 1st revised manuscript 'PDF and CDF of (a) DT and (b) NT in the summer. Red ~' had some type error which is not '(a) DT and (b) NT' but '(a) D_m and (b) $\log_{10}(N_w)$'. Therefore, explanations in the caption of Figure 12c in the present manuscript are little different with the Figure 14b in the previous manuscript.

• The reference to Waldvogel (1974) seems to be not used and should be removed of the references list.

Author's answer: Thank you for your advice. We removed it.

[Page 31, Line 675-676]

'Waldvogel, A.: The N 0 jump of raindrop spectra, Journal of the Atmospheric Sciences, 31, 1067-1078, 1974' was removed.

Submitted on 05 Oct 2015

Anonymous Referee #2

Overall quality:

The resubmitted version of the manuscript by Suh et al. entitled "Climatological Characteristics of Raindrop Size Distributions in Busan, Korea" has definitely improved in quality as compared to the previous submission. There are still a number of small issues that have to be accounted for before this work can be accepted for publication (see comments below). Furthermore, I would suggest the authors to have the manuscript edited by a native English speaker, as quite a number of sentences are either spelled wrong or difficult to follow.

Author's answer:

The manuscript was edited by a native English speaker before submission. However, we read whole the manuscript carefully and rechecked the misspelled words and expression.

Major concerns:

Page 5 lines 108-109: "Furthermore, … rain rates." I do not understand this sentence as I have the feeling that this statement also holds for a non-normalized DSD.. Please rephrase.

Author's answer: Thank you for your comment. We modified it as follows;

[Page 5, Line 108-109]

'Furthermore, a normalized gamma DSD enables the quantitative comparison for rainfall cases regardless of time scale and rain rate.**'**

Page 17 lines 347-350: This sentence is very unclear. But since the authors refer to a figure which is not presented in the manuscript, I would suggest to remove these lines from the text.

Author's answer: Thank you for your comment and we are sorry to make you feel confusing. What we want to say is that the average value of $\log_{10}(N_w)$ for each rainfall type is larger than the reference line when D_m is greater than 1.7 mm (figure not shown), which is similar to the result of Järvenpää, Finland (Fig.14 of Leinonen et al., 2012). However, we removed this sentence to avoid confusing according to the Referee's recommendation.

[Page 17, Line 358-360]

'However, the average line of $\log_{10}(N_w)$ for each rainfall type extends beyond the reference line when D_m is greater than 1.7 mm (figure not shown), which is similar to the results from Järvenpää, Finland (Fig.14 of Leinonen et al., 2012).**'** was removed.

Figure 6: Change the legend symbols of "Daytime" and "Nighttime" in the bottom panel into a "+" sign instead of using the "o" symbol.

Author's answer: Thank you for your comment and we feel sorry to make you confused. The result of present study includes daytime as well as nighttime. The 'o' sign is the present study result and '+' sign is the result of previous study (Bringi et al., 2003). To avoid confusing, we added the sentence in the caption of Figure 5 as 'These mean values for each rainfall type are shown as circle symbols.'.

[Figure5, Page 42, Line 802]

'(b) Scatter plot of mean D_m and $\log_{10}(N_w)$ values of the 10 rainfall categories with respect to stratiform rainfall and these mean values for each rainfall type are shown as circle symbols. ~'

Page 17 lines 354-355: "The scatter … maritime cluster". I do not agree with this statement. The 1-minute data is all over the place, corresponding to both continental and maritime precipitation.

Author's answer: Thank you for your comment. Of course we completely agreed to your comment. However, our point here is that 'data points are more distributed in continental-like cluster than in maritime-like one'.

[There is no add or modify]

Page 17 line 360 equation 16: This fitted equation is heavily influence by the typhoon outlier. In case this point is not taken into account in Fig. 6B, I expect a completely different result for the fitted line. Therefore, I would suggest that the authors add some more details on the limitations of this fitting procedure on page 17.

Author's answer: Thank you for your idea. We added the limitations in the manuscript as follows;

[Page 18, Line 372-373]

'Even the coefficients in Equation 16 might be changed slightly with the Typhoon values, this result does not represent in D_m < 1.2 mm and D_m > 1.9 mm'

Page 21 line 453: Please rephrase "It is .. with R."

Author's answer: Thank you for your comment and we modified it as follows;

[Page 22, Line 465-467]

'The diurnal variation of rain rate in the present study from 0200 (1200) KST to 1000 (2000) KST shows relatively smaller (larger) frequencies of sea wind. It is different pattern with the result of Kozu et al. (2006).'

Page 23 lines 453-454: Please rephrase "Bringi et al. … D_m and N_w"

Author's answer: Thank you for your comment. We modified it as follows;

[Page 23, Line 495-496]

'Bringi et al. (2003) referred that the convective rainfall type is able to be classified as the continental and maritime-like precipitation using D_m and N_w'

Page 24 lines 509-510: Please rephrase "except for heavy ... the Typhoon category.

Author's answer: Thank you for your idea. We corrected it as follows;

[Page 24, Line 524-527]

'The mean values of D_m and N_w for stratiform rainfall are relatively small compared with the average line of stratiform rainfall produced by Bringi et al. (2003), except for heavy rainfall events. In case of convective type, mean values of D_m and N_w are converged around the maritime cluster, except for the Typhoon category.'

Page 24 lines 515-521: This information is too specific for a summary and conclusions as these results can be found in the results section of the manuscript. Please try to summarize this part, without being too specific.

Author's answer: Thank you for your comment. We removed unnecessary expressions and modified as follows;

[Page 25, Line 536-540]

'The analysis of diurnal variation in DSD yielded the following results: first, the frequency of μ is higher at NT than during the DT in the negative value. The PDF of R is higher at NT than during the DT when $\log_{10}(R) > 0.6$. The value of PDF for D_m during DT is larger than NT smaller than 0.65 mm. For N_w, which tends to be inversely related to D_m, its frequency is higher at NT than DT when $\log_{10}(N_w) > 3.8$.'

Minor concerns:

Page 2 line 28: Change "cover" into "convering" and add "also" after ", but"

Author's answer: Thank you for your comment. We changed as Referee's comment.

[Page 2, Line 28]

'~ 10 categories not only covering different temporal and spatial scales, but also different rainfall types.'

Page 2 line 29: Change “value” into “values”

Author’s answer: Thank you for your comment. We modified it.

[Page 2, Line 29]

‘When only convective rainfall was considered, mean values of ~’

Page 9 line 176-177: Change “does not consider because of beyond the research.” into “was not considered because it lies beyond this work.”

Author’s answer: Thank you for your idea. We modified it as Referee’s comment.

[Page 9, Line 178-179]

‘~ was not considered because it lies beyond this work.’

Page 15 line 305: Change “infer” into “inferred”

Author’s answer: Thank you for your comment. We changed it as Referee’s comment.

[Page 15, Line 315]

‘It is inferred that the similar ~’

Page 15 line 314: Change “distribute” into “distributed”

Author’s answer: Thank you for your advice. We changed it as Referee’s comment.

[Page 16, Line 324]

‘~ (Fig. 4f) is widely distributed between ~’

Page 18 line 375: Change “higher in the” into “more ofter observed during”

Author’s answer: Thank you for your comment. We changed it as Referee’s comment.

[Page 19, Line 387]

‘~ more often observed during ~’

Page 23 line 499: Change “error” into “errors”

Author’s answer: Thank you for your comment. We changed it as Referee’s comment.

[Page 24, Line 516]

‘to remove errors by performing ~’

Page 24 line 514: Change “display” into “displays”

Author’s answer: Thank you for your advice. We changed it as Referee’s comment.

[Page 25, Line 534]

‘~ associated with convective rainfall displays a linear ~’

Page 24 line 523: Change “is correspond” into “corresponds”

Author’s answer: Thank you for your comment. We corrected it as Referee’s comment.

[Page 26, Line 548]

‘Smaller D_m corresponds to the large ~’

Page 25 line 524-525: Remove “based on … wind direction.”

Author’s answer: Thank you for your comment. This is the final result of the present study. Therefore, we modified them from ‘, based on the results of Bringi et al. (2003) and wind direction.’ to ‘according to the features of wind’

[Page 26, Line 550]

‘~ than in the NT (DT) according to the features of wind.’

Climatological Characteristics of Raindrop Size Distributions in Busan, Korea

Sung-Ho SUH[1]

Cheol-Hwan YOU[2*]

Email: youch@pknu.ac.kr

Dong-In LEE[1,2]

Institutional addresses:

[1] Department of Environmental Atmospheric Sciences, Pukyong National University, Daeyeon campus 45, Yongso-ro, Namgu, Busan 608-737 Republic of Korea

[2]Atmospheric Environmental Research Institute, Daeyeon campus 45, Yongso-ro, Namgu, Busan 608-737 Republic of Korea

* Corresponding author

Abstract

Raindrop size distribution (DSD) characteristics within the complex area of Busan, Korea (35.12°N, 129.10°E) were studied using a Precipitation Occurrence Sensor System (POSS) disdrometer over a four-year period from February 24th 2001 to December 24th 2004. Also, to find the dominant characteristics of polarized radar parameters which is differential radar reflectivity (Z_{dr}), specific differential phase (K_{dp}) and specific attenuation (A_h), T-matrix scattering simulation was applied in present study. To analyze the climatological DSD characteristics in more detail, the entire period of recorded rainfall was divided into 10 categories not only covering different temporal and spatial scales, but also different rainfall types. When only convective rainfall was considered, mean values of mass weighted mean diameter (D_m) and normalized number concentration (N_w) values for all these categories converged around a maritime cluster, except for rainfall associated with Typhoons. The convective rainfall of a Typhoon showed much smaller D_m and larger N_w compared with the other rainfall categories.

In terms of diurnal DSD variability, we observe maritime (continental) precipitation during the daytime (DT) (nighttime, NT), which likely results from sea (land) wind identified through wind direction analysis. These features also appeared in the seasonal diurnal distribution. The DT and NT Probability Density Function (PDF) during the Summer was similar to the PDF of the entire study period. However, the DT and NT PDF during the Winter season displayed an inverse distribution due to seasonal differences in wind direction.

Keyword: DSD, POSS disdrometer, Climatological characteristics, Land and sea wind.

1. Introduction

Drop Size Distribution (DSD) is controlled by the microphysical processes of rainfall and therefore plays an important role in the development of quantitative rainfall estimation algorithms based on forward scattering simulations of radar measurements (Seliga and Bringi, 1976). DSD data accurately reflect local rainfall characteristics within an observation area (You et al., 2014). Many DSD models have been developed to characterize spatial-temporal differences in DSDs under various atmospheric conditions (Ulbrich, 1983). Marshall and Palmer (1948) developed an exponential DSD model using DSD data collected by a filter paper technique ($N(D) = 8 \times 10^3 \exp(-410R^{-0.21}D)$ in $m^{-3}mm^{-1}$, D in mm and R in mm h^{-1}). In subsequent studies, a lognormal distribution was assumed to overcome the problem of exponential DSD mismatching with real data (Mueller, 1966; Levin, 1971; Markowitz, 1976; Feingold and Levin, 1986).

To further investigate natural DSD variations, Ulbrich (1983) developed a gamma DSD that permitted changing the dimension of the intercept parameter (N_0 in $m^{-3}\ mm^{-1-\mu}$) with ($N(D) = N_0 D^{\mu} \exp(-\Lambda D)$). In addition, to enable the quantitative analysis of different rainfall events, the development of a normalized gamma DSD model that accounted for the independent distribution of DSD from the disdrometer channel interval enabled a better representation of the actual DSD (Willis, 1984; Dou et al., 1999; Testud et al., 2001).

DSDs depend on the rainfall type, geographical and atmospheric conditions, and observation time, and are closely linked to microphysical characteristics that control rainfall development mechanisms. In the case of stratiform rainfall, raindrops grow by accretion because of the relatively long residence time in weak updrafts, in which almost all water droplets are changed to ice particles. With time, the ice particles grow sufficiently and fall to the ground. The

raindrop size of stratiform rainfall observed at the ground level is larger than that of convective rainfall for a same rainfall rate due to the resistance of the ice particles to break-up mechanisms. In contrast to stratiform rainfall, in convective rainfall raindrops grow by the collision-coalescence mechanism associated with relatively strong vertical wind speeds and short residence time in the cloud. Fully-grown raindrops of maritime precipitation are smaller in diameter than those in stratiform rainfall due to the break-up mechanism in case of same rainfall rate (Mapes and Houze Jr, 1993; Tokay and Short, 1996). Convective rainfall can be classified into two types based on the origin and direction of movement. Rainfall systems occurring over ocean and land are referred to as maritime and continental rainfall, respectively (Göke et al., 2007). Continental rainfall is related to a cold-rain mechanism whereby raindrops grow in the form of ice particles. In contrast, maritime rainfall is related to a warm-rain mechanism whereby raindrops grow by the collision-coalescence mechanism. Therefore, the mass-weighted drop diameter (D_m) of continental rainfall observed on the ground is larger than that of maritime rainfall, and a smaller normalized intercept parameter (N_w) is observed in continental rainfall (Bringi et al., 2003).

Specific heat is a major climatological feature that creates differences between DSDs in maritime and continental regions. These two regions have different thermal capacities and thus display different temperature variations with time. The surface temperature of the ocean changes slowly because of the water's high thermal capacity, while the continental regions, which have comparatively lower thermal capacity, display greater diurnal variability. Sea winds generally is occurred in from afternoon to early evening when the temperature gradient between the sea and land becomes negative, which is the opposite of the gradient in the daytime (DT). In coastal regions, the land and sea wind effect causes a pronounced difference between the DT and nighttime (NT) DSD characteristics. Also, when mountains are located near the coast, the

89 difference is intensified by mountain and valley winds (Qian, 2008).

90 In the present study, we analyzed a four-year dataset spanning from 2001 to 2004, collected
91 from Busan, Korea (35.12°N, 129.10°E) using a Precipitation Occurrence Sensor System
92 (POSS) disdrometer, to investigate the characteristics of DSDs in Busan, Korea which consist
93 complex mid-latitude region comprising both land and ocean. To quantify the effect of land
94 and sea wind on these characteristics, we also analyzed diurnal variations in DSDs. The
95 remainder of the manuscript is organized as follows. In Section 2 we review the normalized
96 gamma model and explain the DSD quality control method and the classification of rainfall. In
97 Section 3 we report the results of DSD analysis with respect to stratiform/convective and
98 continental/maritime rainfall, and discuss diurnal variations. Finally, a summary of the results
99 and the main conclusions are presented in Section 4.

100

101 **2. Data and Methods**

102 **2.1. Normalized Gamma DSD**

103 The DSD is defined by $N(D) = N_0 \exp(-\Lambda D)$ $(m^{-3}mm^{-1})$ and the one of the methods to
104 reflect the microphysical characteristics of rainfall using the number concentration of rainfall
105 drops. Also, DSD is able to calculate the many kind of parameters which show the dominant
106 feature of raindrops. Normalization is used to define the DSD and to solve the non-
107 independence of each DSD parameter (Willis, 1984; Dou et al., 1999; Testud et al., 2001).
108 Furthermore, a normalized gamma DSD enables the quantitative comparison for rainfall cases
109 regardless of time scale and rain rate.~~Furthermore, a normalized gamma DSD enables the~~
110 ~~comparison of quantitative estimations for cases of rainfall events that have different time~~
111 ~~scales and rain rates.~~ Here, we use the DSD model designed by Testud et al. (2001):

$$N(D) = N_w f(\mu)\left(\frac{D}{D_m}\right)^{\mu} \exp\left[-(4+\mu)\frac{D}{D_m}\right]. \quad (1)$$

where D is volume equivalent spherical raindrop size (mm), and $f(\mu)$ is defined using the DSD model shape parameter (μ) and gamma function (Γ) as follows:

$$f(\mu) = \frac{6}{4^4}\frac{(\mu+4)^{4+\mu}}{\Gamma(4+\mu)}. \quad (2)$$

From the value of $N(D)$, the median volume diameter (D_0 in mm) can be obtained as follows:

$$\int_0^{D_0} D^3 N(D) dD = \frac{1}{2}\int_0^{D_{max}} D^3 N(D) dD. \quad (3)$$

Mass-weighted mean diameter (D_m in mm) is calculated as the ratio of the fourth to the third moment of the DSD:

$$D_m = \frac{\int_0^{D_{max}} D^4 N(D) dD}{\int_0^{D_{max}} D^3 N(D) dD}. \quad (4)$$

129 The normalized intercept parameter (N_w in $m^{-3}mm^{-1}$) is calculated as follows:

130

131 $$N_w = \frac{4^4}{\pi \rho_w}\left(\frac{LWC}{D_m^4}\right). \quad (5)$$

132

133 The shape of the DSD is calculated as the ratio of D_m to the standard deviation (SD) of D_m

134 (σ_m in mm) (Ulbrich and Atlas, 1998; Bringi et al., 2003; Leinonen et al., 2012):

135

136 $$\sigma_m = \left[\frac{\int_0^{D_{max}} D^3 (D - D_m)^2 N(D) dD}{\int_0^{D_{max}} D^3 N(D) dD}\right]^{\frac{1}{2}}. \quad (6)$$

137

138 In addition, σ_m / D_m is related to μ as follows:

139

140 $$\frac{\sigma_m}{D_m} = \frac{1}{(4+\mu)^{1/2}}. \quad (7)$$

141

142 Liquid water content (LWC in g m^{-3}) can be defined from the estimated DSD:

143

144 $$LWC = \frac{\pi}{6} \rho_w \int_0^{D_{max}} D^3 N(D) dD. \quad (8)$$

145

where ρ_w is water density ($g\,m^{-3}$) and it assumed as 1×10^{6}~~1~~ $g\,m^{-3}$ for a liquid water. Similarly, rainfall rate (R in $mm\,h^{-1}$) can be defined as follows:

$$R = \frac{3.6}{10^3}\frac{\pi}{6}\int_0^{D_{max}} v(D)D^3N(D)dD. \quad (9)$$

where the value of factor 3.6×10^3 is the unit conversion which converts the mass flux ~~unis~~ unit ($mg\,m^{-2}\,s^{-1}$) to the common unit ($mm\,h^{-1}$) for the convenience. $v(D)$ ($m\,s^{-1}$) is the fall velocity for each raindrop size. The relationship between $v(D)$ and equivalent spherical raindrop size (D in mm) is given by Atlas et al. (1973) who developed an empirical formula based on the data reported by Gunn and Kinzer (1949):

$$v(D) = 9.65 - 10.3\exp[-0.6D]. \quad (10)$$

2.2 Quality Control of POSS Data

POSS was used to measure the number of raindrops within the diameter range of 0.34-5.34 mm, using bistatic, continuous wave X-band Doppler radar (10.525 GHz) across 34 channels (Fig. 1; Sheppard and Joe, 2008). ~~Using~~ To estimate~~d~~ DSD, Doppler power density spectrum is generated as follows;

$$S(f) = \int_{D_{min}}^{D_{max}} N(D_m)V(D_m, \rho, h, w)\bar{S}(f, D_m, \rho, h, w)dD_m. \quad (11)$$

Where $S(f)$ means Doppler spectrum power density, $V(D_m, \rho, h, w)\bar{S}(f, D_m, \rho, h, w)$ means weighting function of $S(f)$, $\bar{S}$ is the mean of $S(f)$, ρ is density of precipitation distribution, h is the shape of precipitation distribution, $w\,(m\,s^{-1})$ is wind speed and $V(x)$ is sample volume and the symbol 'x' means arbitrary parameters which affect the sampling volume. ~~A~~ The Doppler power density spectrum has a resolution of 16Hz and terminal velocity (v_t) has a resolution of 0.24 $m\,s^{-1}$. Transmitter and receiver skewed about 20° toward each other, and cross point of signal is located over 34 cm from transmitter-receiver. Transmitter-receiver toward upper side detects $N(D)$ of raindrops in observation volume ($V(D)$) (Sheppard, 1990). Also, Sheppard (1990) and Sheppard and Joe (1994) noted some shortcomings as the overestimation of small drops at horizontal wind larger than 6 $m\,s^{-1}$. However, in present study, the quality control of POSS for wind effect was not considered because it lies beyond this work.~~does not consider because of beyond the research.~~ Detailed specifications and measurement range and raindrop size for each observation channel of the POSS disdrometer are summarized in Table 1.

A POSS disdrometer was installed in Busan, Korea (35.12°N, 129.10°E), along with other atmospheric instruments, the locations of which are shown in Fig. 2. Estimating raindrop size correctly is challenging and care should be taken to ensure reliable data are collected. We performed the following quality controls to optimize the accuracy of the disdrometer estimates. i) Non-liquid type event data (e.g., snow, hail etc.) detected by POSS were excluded, to focus only on liquid state rainfall. ii) DSD spectra in which drops were not found in at least five

consecutive channels were removed as non-atmospheric. ~~ii) Non-atmospheric data were removed from the analysis if the number of DSD spectra was smaller than five consecutive channels, or the position of DSD spectra only detected in smaller (larger) than the 5th (10th) channel for each 1-min channel data.~~ iii) Only data recorded in more than 10 complete channels were considered. iv) To compensate for the reduced capability to detect raindrops smaller than 1 mm when R > 200 mm h^{-1} (as recorded by the disdrometer), data collected when R > 200 mm h^{-1} were not included in the analyses. v) To eliminate wind and acoustic noise, data collected when R < 0.1 mm h^{-1} were removed (Tokay and Short, 1996). vi) The value of D_0 which is calculated by Eq. (3) tends to be overestimated when D_0 < 0.5 mm (Leinonen et al., 2012). Because the correlation coefficient between D_0 and D_m was 0.985 for the whole study period, we considered that D_m could be used for the analysis instead of D_0.

After performing all quality control procedures, 99,388 spectra were left from an original total of 166,682 for 1-min temporal resolution. Accumulated rainfall amount from POSS during the entire period was 4261.49 mm. To verify the reliability of the POSS data, they were compared with data collected by a 0.5 mm tipping bucket rain gaugeat an automatic weather system (AWS) located ~368 m from the POSS (Fig. 3).

2.3 Radar Parameters

~~To derive the rainfall relations, polarized parameters were computed by a T-matrix scattering simulation (Waterman, 1971; Zhang et al., 2001).~~ First, the radar reflectivity factor (z, mm^6m^{-3}) and non-polarized radar reflectivity (Z, dBZ) were computed using the DSD data collected by POSS, as follows:

$$z = \int_0^{D_{max}} D^6 N(D) dD. \quad (12)$$

$$Z = 10\log_{10}(z). \quad (13)$$

The T-matrix method used in this study is initially proposed by Waterman (1965, 1971) to calculate electromagnetic scattering by single non-spherical raindrops. The adaptable parameters for this calculation are frequency, temperature, hydrometeor types, raindrop's canting angle and drop axis ratio and explained the following sentences. Axis ratios of raindrops differ with atmospheric conditions and rainfall type. To derive the drop shape relation from the drop diameter, we applied the results of numerical simulations and wind tunnel tests employing a forth-polynomial equation, as in many previous studies (Beard and Chuang, 1987; Pruppacher and Beard, 1970; Andsager et al., 1999; Brandes et al., 2002). The drop-shape relation used in the present study is a combination of those from Andsager et al. (1999) and Beard and Chuang (1987) for three raindrop size ranges (Bringi et al., 2003).

The raindrop axis ratio relation of Andsager et al. (1999) is applied in the range of $1 < D\,(\mathrm{mm}) < 4$, as follows:

$$r = 1.0048 + 0.0057D - 2.628D^2 + 3.682D^3 - 1.677D^4. \quad (14)$$

The drop-shape relation of Beard and Chuang (1987) is applied in the range of $D < 1$ mm

231 and $D > 4$ mm, as follows:

232

233 $$r = 1.012 + 0.01445D - 0.01028D^2. \quad (15)$$

234

235 We assumed SD and the mean canting angle of raindrops as 7° and 0°, respectively. The
236 refractive indices of liquid water at 20 ℃ were used (Ray, 1972). Also, the condition of
237 frequency for electromagnetic wave of radar is 2.85 GHz (S-band). We calculated dual
238 polarized radar parameters based on these conditions. The parameters of differential reflectivity,
239 Z_{dr} (dB), specific differential phase, K_{dp} ($\deg km^{-1}$), and attenuation, A_h ($dB\,km^{-1}$),
240 using DSD data were calculated and analyzed.

241

242 **2.4. Classification of Rainfall Types and Rainfall Events**

243 Rainfall systems can be classified as stratiform or convective in nature, via analysis of the
244 following microphysical characteristics: i) DSD, using relationships between N_0 and R (N_0 ~~=~~
245 $> 4 \times 10^9 R^{4.3}$ in $m^{-3}mm^{-1}$ is considered as convective rainfall, ~~(~~Tokay and Short, 1996;
246 Testud et al., 2001); ii) radar reflectivity, where, according to Gamache and Houze (1982), a
247 rainfall system that displays radar reflectivity larger than 38 dBZ is considered to be
248 convective; and iii) rainfall rate, where average value larger than 0.5 mm per 5 min~~5 min R >~~
249 ~~0.5 mm h^{-1}~~ is considered as convective rainfall (Johnson and Hamilton, 1988). Alternatively,
250 rainfall that has 1-min $R > 5$ (0.5) $mm\,h^{-1}$ and a SD of $R >$ (<) 1.5 $mm\,h^{-1}$ is considered
251 as convective (stratiform) type (Bringi et al., 2003). The rainfall classification method proposed

by Bringi et al. (2003) is applied in the present study.

It is necessary to categorize different rainfall systems because their microphysical characteristics show great variation depending on the type of rainfall, as well as the type of rainfall event; e.g., Typhoon, ~~Chanma~~Changma, heavy rainfall and seasonally discrete rainfall. To investigate the temporal variation in DSDs, we analyzed daily and seasonal DSDs. Likewise, to investigate diurnal variability in DSD, DT and NT data were considered by using the sunrise and sunset time in Busan (provided by the Korea Astronomy and Space Science Institute [KASI]). In the middle latitudes, and including Busan, the timings of sunrise and sunset vary due to solar culminating height. The earliest and latest sunrise (sunset) time of the entire period is 0509 KST (1712 KST) and 0733 KST (1942 KST), respectively. DT (NT) is defined as the period from the latest sunrise (sunset) time to the earliest sunset (sunrise) time for the unity of classification of each time group (Table 2).

To analyze the predominant characteristics of DSDs for Typhoon rainfall, nine Typhoon events were selected from throughout the entire study period which is summarized in Table 2.

This study utilizes the Korea Meteorological Administration (KMA) rainfall warning regulations to identify heavy rainfall events. The KMA issues a warning if the accumulated rain amount is expected to be >70 mm within a 6-hour period, or >110 mm within a 12-hour period. Rainfall events classified as ~~Chanma~~Changma and Typhoon were not included in the classification 'heavy rainfall'.

~~Chanma~~Changma is the localized rainfall system or rainy season that is usually present over the Korean Peninsula between mid-June and mid-July which is similar to the Meiyu (China) or Baiu (Japan). The selected dates and periods of each rainfall category are summarized in Table 2.

3. Results

3.1. DSD and Radar Parameters

Figure 4 shows the Probability Density Function (PDF) and Cumulative Distribution Function (CDF) of DSDs and radar parameters with respect to stratiform and convective rainfall. The PDFs of DSD and radar parameters were calculated using the non-parameterization kernel estimation to identify the dominant distribution of each parameter recorded in Busan. Non-parameterization kernel estimation was also used to identify continuous distributions of DSDs. The PDF of stratiform rainfall is more similar to that of the dataset for the entire analysis period due to the dominant contribution of stratiform rainfall (about 62.93%) to the overall rainfall than that of convective rainfall. However, the PDF for convective rainfall is significantly different from that of the entire analysis period, and as the convective rainfall contributes only 6.11% of the overall rainfall (Table 3). When $\mu < 0$ the distribution of μ for convective rain has more value of PDF than that for stratiform rain (Fig. 4a). Alternatively, the frequency of μ for stratiform rainfall is higher than that of convective rainfall when $0 < \mu \geq\!\!\!< 5$. The value of μ for convective rainfall is higher than that for stratiform rainfall because the break-up mechanism would be increase the number concentration of small raindrops. The number concentrations of mid-size raindrops increased due to the decrease in the number concentration of relatively large raindrops (Hu and Srivastava, 1995; Sauvageot and Lacaux, 1995). However, we observed a higher frequency of convective rainfall than stratiform rainfall in the negative μ range.

296 The PDF of D_m displays peak around 1.2 and 1.4 mm for stratiform rainfall and the entire
297 rainfall dataset, respectively. We note that a gentle peak exists around 0.7 mm for both
298 stratiform and convective rainfall datasets (Fig. 4b). These features are similar to the
299 distribution of D_m observed in a high-latitude region at Järvenpää, Finland (Fig. 4 of Leinonen
300 et al., 2012). For D_m values > 1.7 mm, the PDF for convective rainfall is higher than
301 stratiform rainfall. Accordingly, the value of DSD for stratiform rainfall is higher than that of
302 convective rainfall when D_m < 1.7 mm. Generally, stratiform rainfall that develops by the
303 cold rain process displays weaker upward winds and less efficient break-up of raindrops.
304 Therefore, in the same rainfall rate, stratiform rainfall tends to produce larger raindrops than
305 convective rainfall that develops by the warm rain process. However, the average D_m values
306 for convective and stratiform rain for the entire period are approximately 1.45 and 1.7 mm,
307 respectively. In short, D_m is proportional to R regardless of rainfall type. This finding is
308 consistent with the results of Atlas et al. (1999) who found that the D_m of convective rainfall
309 is larger than that of stratiform rainfall on Kapingamarangi Island, Micronesia.
310 The PDF of $\log_{10}(N_w)$ for the entire rainfall dataset was evenly distributed between 1.5 and
311 5.5, with a peak at N_w = 3.3 (Fig. 4c). The PDF of $\log_{10}(N_w)$ for stratiform rainfall is rarely
312 > 5.5, while for convective rainfall it is higher at > 5.5 than that of stratiform. There is a similar
313 frequency in the stratiform and convective rainfall at 4.4
314 The PDF distributions for $\log_{10}(R)$ and $\log_{10}(LWC)$ are similar each other (Fig. 4d and e).
315 It is inferred that the similar results come from the using of alike moment of DSD as 3.67 and
316 3 for R and LWC, respectively. The PDF of $\log_{10}(R)$ for the entire rainfall dataset ranged
317 between -0.5 and 2. A peak exists at 0.3 and the PDF rapidly decreases from the peak value as
318 R increases. The PDF for stratiform rainfall has a higher frequency than that of the entire

rainfall when -0.3 < $\log_{10}(R)$ < 0.7, while the PDF for convective rainfall is denser between 0.4 and 2. Furthermore, the frequency of the PDF for convective rainfall was higher than that of stratiform rainfall in case of $\log_{10}(R)$ > 0.65 and the peak value shown was 0.9.

The PDF and CDF for non-polarized reflectivity (Z), differential reflectivity (Z_{dr}), specific differential phase (K_{dp}), and specific attenuation of horizontal reflectivity (A_h) are shown in Fig. 4f-i. The PDF of Z_h for stratiform rainfall (Fig. 4f) is widely distributed between 10 and 50 dBZ with the peak at approximately 27 dBZ. Conversely, for convective rainfall, the value of PDF lie between 27 and 55 dBZ and the peak frequency value at approximately 41 dBZ. The frequency value of reflectivity is higher for convective rainfall than for stratiform rainfall in the range of ~ >35 dBZ. Furthermore, the shape of the PDF for convective rainfall is similar to that reported for Darwin, Australia (Steiner et al., 1995); however, for stratiform rainfall there are significant differences between Busan and Darwin in terms of the shape of the frequency distribution. The PDF of Z_{dr} for the entire rainfall primarily exists between 0 and 2.5 dB, and the peaks are at 0.3 and 1.8 dB (Fig. 4g). The distribution of Z_{dr} for convective and stratiform rainfall is concentrated between 0.6 and 1.6 dB, and between 0.3 and 2 dB, respectively. The frequency of Z_{dr} for convective (stratiform) rainfall exists in ranges higher (lower) than stratiform (convective) at 0.9 dB.

The dominant distribution of K_{dp} for the entire dataset and for stratiform rainfall lies between 0 and 0.14 deg km^{-1}, with a peak value of 0.03 deg km^{-1} and 0.08 deg km^{-1}. However, for convective rainfall the PDF of K_{dp} is evenly exist between 0.01 and 0.15 deg km^{-1}. Furthermore, when K_{dp} > 0.056 deg km^{-1}, the frequency of the PDF for convective rainfall is higher than that of stratiform rainfall (Fig. 4h).

The PDF of A_h is similar to that of K_{dp} and is exist between 0 and 0.01 dB km^{-1}. For the

case of the entire rainfall dataset and for stratiform rainfall, the PDF of A_h is concentrated between 0 and 2.0×10^{-3} dB km^{-1} and that of convective rainfall is strongly concentrated between 1.0×10^{-3} and 8.0×10^{-3} dB km^{-1} (Fig. 4i). Unlike the PDF of A_h for convective rainfall, the PDF for stratiform rainfall shows a strong peak at about 7.0×10^{-4} dB km^{-1}.

3.2. Climatological Characteristics of DSD in Busan

The climatological characteristics of DSDs for 10 rainfall categories are analyzed in this study. Sample size and ratio rainfall for each category are summarized in Table 3. Figure 5a illustrates the distribution of all 1-min stratiform rainfall data, and Fig. 5b shows scatter plots of averaged D_m and $\log_{10}(N_w)$ for all 10 rainfall categories for stratiform rainfall data. Figure 5a displays a remarkable clear boundary in the bottom sector and shows that most of the data lie below the reference line used by Bringi et al. (2003) to classify convective and stratiform rainfall. The average value of D_m and $\log_{10}(N_w)$ for all rainfall categories, except for heavy rainfall, exist between 1.4 and 1.6 mm and between 3.15 ~~to~~ and 3.5~~-~~, respectively (Fig. 5b). These values are relatively small compared with the reference line presented by Bringi et al. (2003). ~~However, the average line of $\log_{10}(N_w)$ for each rainfall type extends beyond the reference line when D_m is greater than 1.7 mm (figure not shown), which is similar to the results from Järvenpää, Finland (Fig.14 of Leinonen et al., 2012).~~

The distribution of 1-min convective rainfall data is displayed in Fig. 6a and the distribution of average values of D_m and N_w for the 10 rainfall categories in the case of convective rainfall in Fig. 6b. The blue and red plus symbols represent maritime and continental rainfall, respectively, as defined by Bringi et al. (2003). The scatter plot of 1-min convective rainfall

data shows more in the continental cluster than the maritime cluster; however, the average values for the 10 rainfall categories are all located around the maritime cluster, except for the Typhoon category. By considering the entire average values including Typhoon event (Fig. 6b), we can induce the simple linear equation using D_m and $\log_{10}(N_w)$ as follows:

$$\log_{10}(N_w) = -1.8D_m + 6.9. \quad (16)$$

Even the coefficients in Equation 16 might be changed slightly with the Typhoon values, this result does not represent in D_m < 1.2 mm and D_m > 1.9 mm. The D_m (N_w) value for the Typhoon category was considerably smaller (larger) than that of the other categories as well as that of stratiform type of Typhoon. This result does not agree with that reported by Chang et al. (2009), who noted that the D_m of convective rainfall Typhoon showed a large value compared with that associated with stratiform rainfall.

3.3 Diurnal Variation in Raindrop Size Distributions

3.3.1. Diurnal Variations in DSDs

Figure 7a shows a histogram of normalized frequency of 16 wind directions recorded by the AWS, which is the same instrument as that used to collect the data shown in Fig. 3. To establish the existence of a land and sea wind, the difference in wind direction frequencies between DT and NT were analyzed. Figure 7b shows the difference between DT and NT, difference frequency means normalized frequency of wind direction for DT subtract to that of NT for each direction, in terms of the normalized frequency of 16 wind directions. In other word, positive

(negative) values indicate that the frequency of wind is ~~higher in the~~more often observed during DT (NT). Also, land (sea) wind defined in present study from 225° (45°) to 45° (225°) according to the geographical condition in Busan. The predominant frequency of wind direction in the DT (NT), between 205° (22.5°) and 22.5° (205.5°), is higher than that in the NT (DT) (Fig. 7b). The observation site where the POSS was installed at western side from the closest coast line, distance is about 611 m, suggesting that the effect of the land and sea wind would have been recorded.

To understand the effects of the land and sea wind on DSD characteristics, we analyzed the PDF and 2-hour averaged DSD parameters for DT and NT. Figure 8 illustrates the distributions of μ, D_m, $\log_{10}(N_w)$, $\log_{10}(LWC)$, $\log_{10}(R)$, and Z. There were large variations of μ with time. The μ values varied from 2.41 to 3.17 and the minimum and maximum μ values occurred at 0800 KST and 1200 KST, respectively (Fig. 8a). A D_m larger than 1.3 mm dominated from 0000 KST to 1200 KST, before decreasing remarkably between 1200 and 1400 KST. The minimum and maximum D_m appeared at 1400 KST and 0800 KST, respectively (Fig. 8b).

N_w generally varies inversely to D_m; however, no inverse relationship was identified between D_m and N_w in case of the time series (Fig. 8c). The maximum and minimum values of N_w were found at 0600 KST and 2200 KST.

Variability through time was similar for R, LWC, and Z_h as D_m. There was an increasing trend from 0000 KST to 0800 KST followed by a remarkably decreasing trend from 0800 KST to 1400 KST (Figs 8d, 11e and 11f). Note that the time of the sharp decline for R between 1200 KST and 1400 KST is simultaneous with a D_m decrease. Larger (smaller) drops would contribute to higher R in the morning (afternoon). These variations considerably matched

410 with the diurnal sea wind time series (Fig. 8g). Sea wind is the sum value of normalized wind
411 frequency between 45° and 225°. From 0200 (1400) KST to 1200 (2000) KST shows smaller
412 (larger) value of sea wind frequency which is opposite to the relatively larger (smaller) parts of
413 each parameter (D_m, R, LWC and Z_h).
414 The PDF distribution of μ between -2 and 0 is more concentrated for NT than for DT.
415 Furthermore, when μ > 0, DT and NT frequency distributions are similar (Fig. 9a). A larger
416 $N(D)$ of small or large raindrops would be expected in NT than in DT.
417 The distribution of DT D_m < 0.7 mm is wider than that of the NT. However, between 0.7
418 and 1.5 mm the frequency for NT is higher than that for DT, whereas the distribution in the
419 range > 1.5 mm is similar for both DT and NT (Fig. 9b). We note that the smaller peak of D_m
420 around 0.6 mm for the entire rainfall dataset (Fig. 4b) was observed only in DT.
421 The distribution of $log_{10}(N_w)$ for DT has higher value of PDF at larger $log_{10}(N_w)$ than that
422 of NT at $log_{10}(N_w)$ > 4 (Fig. 9c).
423 Bringi et al. (2003) noted that the maritime climatology displayed larger N_w and smaller D_m
424 values than the continental climatology, based on observed DSDs in the low and middle latitude.
425 Also, Göke et al. (2007) emphasized that rainfall type can be defined by the origin location and
426 movement direction. In accordance with these previous results, we consider NT rainfall in the
427 Busan region to be more likely caused by a continental convective system.
428 In the present study, the shape of the PDF of LWC and R for DT and NT are similar which is
429 the same reason with the results of Fig. 4e-f. LWC and R distributionss during the DT (NT)
430 are higher (lower) than in the NT (DT) when $log_{10}(LWC)$ and $log_{10}(R)$ are larger (smaller)
431 than -1.2 and 0–, respectively (Fig. 9d and e). The Z has similar pattern with LWC and R
432 during the DT (NT) was higher (lower) than in the NT (DT) in the range below (above) about

27 dBZ (Fig. 9f).

3.3.2. Diurnal Variations of DSDs with respect to Season

Busan experiences distinct atmospheric conditions that are caused by the different frequencies and magnitudes of land and sea winds in response to variable sunrise and sunset times. To identify seasonal variations of DSDs with respect to the effect of the land and sea wind, we analyzed the DT and NT PDF of D_m and N_w in the Summer and Winter. The start and end times of DT (NT) were sorted using the latest sunrise (sunset) and the earliest sunset (sunrise) time for each season (Table 4) which is same method that of entire period classification.

Figure 10a shows a histogram of wind directions in Summer (light grey) and Winter (dark grey). The frequencies of Summer and Winter wind directions are similar to each other. However, in Fig. 10b, the DT and NT distributions of Winter wind direction display opposing frequencies. Note that Winter season shows remarkable frequency of land (sea) wind between 0° (157.5°) and 45° (202.5°) at DT (NT) compared with results of those for Summer season. The accumulated value of normalized wind frequencies at the sea and land wind show different feature between Summer and Winter season (Table 5).

To identify the variability of DSDs caused by the land and sea wind in Summer and Winter, a 2-hour interval time series of D_m, N_w and R was analyzed. In the Summer, the time series of D_m displays considerably large values between 0000 KST and 1200 KST, compared with the period between 1400 KST and 2200 KST (Fig. 11a). The mean value of D_m decreases dramatically between 1200 KST and 1400 KST. $log_{10}(N_w)$ generally has a negative relationship with D_m (Fig. 11b). However, the inverse relation between $log_{10}(N_w)$ and D_m is not remarkable. The $log_{10}(R)$ tends to increase gradually from 0000 KST to 0800 KST and

456 decrease from 0800 KST to 1400 KST, which is similar to the pattern that of entire period (Fig.
457 11c). Kozu et al. (2006) analyzed the diurnal variation in R at Gadanki (South India),
458 Singapore, and Kototabang (West Sumatra) during the Summer monsoon season. All regions
459 displayed maximum R at approximately 1600 LST, except for Gadanki. Also, Qian (2008),
460 who analyzed the diurnal variability of wind direction and R on Java Island during the
461 Summer season using 30 years (from 1971 to 2000) of NCEP/NCAR reanalyzed data. They
462 found that a land wind occurred from 0100 LST to 1000 LST and a sea wind from 1300 LST
463 to 2200 LST (Fig. 7 of Qian (2008)). Normalized wind frequency for each direction is similar
464 pattern to the results of Qian (2008) but pattern of R is different with that of Kozu et al. (2006).
465 The diurnal variation of rain rate in the present study from 0200 (1200) KST to 1000 (2000)
466 KST shows relatively smaller (larger) frequencies of sea wind. It is different pattern with the
467 result of Kozu et al. (2006).~~From 0200 (1200) KST to 1000 (2000) KST shows relatively~~
468 ~~smaller (larger) frequencies of sea wind. It is different pattern with R.~~ However, these patterns
469 matched with the time series of D_m and $log_{10}(N_w)$. Larger frequency of sea wind direction
470 shows counter-proportional (proportional) relationship to the smaller (larger) frequency of D_m
471 ($log_{10}(N_w)$).
472 Variability of the D_m time series for Winter is the inverse of the Summer time series (Fig. 11a).
473 The mean value of D_m steadily increases from 0000 KST to 1600 KST and then decreases
474 from 1600 KST to 2200 KST. The Winter $log_{10}(N_w)$ time series displays a clear inverse
475 pattern compared with the D_m variation with time and increases from 1600 KST to 0400 KST
476 and then steadily decreases from 0400 KST to 1600 KST (Fig. 11b). The peak of $log_{10}(N_w)$
477 occurs at 0400 KST. However, the time series of $log_{10}(R)$ for Winter season shows similar
478 pattern with that of Summer unlike to another parameters (Fig. 11c). Based on the diurnal

variation of R, the variations of D_m and N_w would be independent to R.

Alike to the D_m and $log_{10}(N_w)$, normalized wind frequency of wind direction for Winter season shows inverse relationship to that of Summer season (Fig. 11d). The value of frequency generally decreases (increases) from 0400 (1400) KST to 1400 (0400) KST. Also, it shows symmetry pattern with that of Summer season.

The PDF distribution of Summer D_m displays a relatively large DT frequency compared with NT when D_m < 1.65 mm, except for the range between 0.6 and 0.9 mm. However, in the range of D_m > 1.65 mm, the NT PDF displays a larger frequency (Fig. 12a). The PDF of $log_{10}(N_w)$ for DT (NT) has a larger frequency than the NT (DT) when $log_{10}(N_w)$ > (<) 3.3 but smaller frequency when $log_{10}(N_w)$ < (>) 3.3 (Fig. 12c).

The DT and NT PDFs of D_m and $log_{10}(N_w)$ during Winter display an inverse distribution to that of Summer. For the PDF of D_m, there is a considerable frequency for NT (DT) when D_m < (>) 1.6 mm (Fig. 12b). The PDF of $log_{10}(N_w)$ of Summer season for NT (DT) is larger than that of the DT when $log_{10}(N_w)$ < (>) 3.5 (Fig. 12d). In the PDF analysis, relatively large (small) D_m and small (large) $log_{10}(N_w)$ are displayed during the NT (DT) when a land wind (sea wind) occurs.

Bringi et al. (2003) referred that the convective rainfall type is able to be classified as the continental and maritime-like precipitation using D_m and N_w.~~Bringi et al. (2003) referred that the convective rainfall type is able to classify as the continental and maritime-like precipitation using D_m and N_w.~~ As the previous study result, we analyzed the PDF of DSDs for Summer and Winter with respect to convective rainfall type. These feature would be shown more clearly in convective type. The convective rainfall type of PDFs of DT and NT for Summer show similar shape of distribution to that of all rainfall type (Fig. 3a). For the PDF of D_m, there is a

more frequency for DT (NT) than NT (DT) when D_m < (>) 2.0 mm except for between 0.7 mm and 1.2 mm (Fig. 13a). The PDF of convective rainfall type's $log_{10}(N_w)$ for DT (NT) has a larger frequency than the NT (DT) when $log_{10}(N_w)$ > (<) 3.4 except for between 4.3 and 5.5 (Fig. 12c). PDF distributions for Winter season show more clear pattern compared with those of the entire rainfall type. The value of PDF for D_m in DT (NT) have considerably larger than NT (DT) when D_m > (<) 1.9 mm, especially between 2.15 mm and 2.3 mm (Fig. 13b). Also, those for $\log_{10}(N_w)$ in DT (NT) show dramatic values when $\log_{10}(N_w)$ < (>) 3.6. Furthermore, PDF values significantly concentrated on between 3 < $\log_{10}(N_w)$ < 3.2 (Fig. 13d). In short, considering the DSD parameters with wind directions, the maritime (continental)-like precipitation would depend on the sea (land) wind.

4. Summary and Conclusion

Climatological characteristics of DSDs in Busan were analyzed using the DSD data observed by POSS over a four-year period from February 24th 2001 to December 24th 2004. Observed DSDs were filtered to remove errors by performing several quality control measures, and an AWS rain gauge installed nearby was used to verify the rainfall amount recorded by the POSS. We analyzed DSD characteristics of convective and stratiform rainfall types, as defined by Bringi et al. (2003). The rainfall dataset was thus divided into stratiform and convective rainfall and their contributions to the total rainfall were 62.93% and 6.11%, respectively. Also, to find the climatological characteristics of DSD for rainfall case, the entire rainfall data was classified as 10 rainfall categories including the entire period case.

According to the study by Bringi et al. (2003), the rainfall in Busan shows maritime climatological DSD characteristics. The mean values of D_m and N_w for stratiform rainfall are

relatively small compared with the average line of stratiform rainfall produced by Bringi et al. (2003), except for heavy rainfall events. In case of convective type, mean values of D_m and N_w are converged around the maritime cluster, except for the Typhoon category. ~~The mean values of D_m and N_w for stratiform rainfall are relatively small compared with the average line of stratiform rainfall produced by Bringi et al. (2003), except for heavy rainfall events and those for convective type converged around the maritime cluster, except for the Typhoon category.~~ The convective rainfall associated with a Typhoon has considerably smaller D_m and larger N_w values compared with the other rainfall categories. This is likely caused by increased raindrop break-up as a result of strong wind effects. Furthermore, the distributions of mean D_m and N_w values for all rainfall categories associated with convective rainfall displays a linear relationship including the Typhoon category.

The analysis of diurnal variation in DSD yielded the following results: first, the frequency of μ is higher at NT than during the DT in the negative value. The PDF of R is higher at NT than during the DT when $\log_{10}(R) > 0.6$. The value of PDF for D_m during DT is larger than NT smaller than 0.65 mm. For N_w, which tends to be inversely related to D_m, its frequency is higher at NT than DT when $\log_{10}(N_w) > 3.8$. ~~The analysis of diurnal variation in DSD yielded the following results: first, in the negative range of μ, the frequency of μ is higher at NT than during the DT. The PDF of R is higher at NT than during the DT when $\log_{10}(R) > 0.6$. A gentle peak of D_m was identified during the DT at approximately 0.6 mm. Additionally, the frequency of D_m is higher at NT than during the DT when $D_m > 0.7$ mm. For N_w, which tends to be inversely related to D_m, its frequency is higher at NT than during the DT when $\log_{10}(N_w) > 4$. At NT, D_m is higher and R, μ, and N_w values are lower compared with the DT.~~ This feature is matched with the time series of normalized frequency of sea wind which

shows inverse relationship to D_m. Smaller D_m ~~is~~ corresponds to the larger sea wind frequency. In short, maritime (continental) –like precipitation are observed in the DT (NT) more often than in the NT (DT) according to the features of wind.~~, based on the results of Bringi et al. (2003) and wind direction.~~ The above-mentioned DSD characteristics are likely due to the land and sea wind caused by differences in specific heat between the land and ocean. These features are also apparent in the seasonal diurnal distribution. The PDF of DT and NT for convective rainfall type during the Summer is similar to the PDF of the entire period; however, those of the Winter displays the significant inverse distribution compared to Summer because of obvious seasonal differences in wind direction.

Author contributions

Cheol-Hwan You designed the study. Sung-Ho Suh modified the original study theme and performed the study. Cheol-Hwan You and Sung-Ho Suh performed research, obtained the results and prepared the manuscript along with contributions from all of the co-authors. Dong-In Lee examined the results and checked the manuscript.

Acknowledgement

This work was funded by the Korea Meteorological Industry Promotion Agency under Grant KMIPA 2015-1050

588

589

590 **References**

591 Andsager, K., Beard, K. V., and Laird, N. F.: Laboratory measurements of axis ratios for large
592 raindrops, Journal of the Atmospheric Sciences, 56, 2673-2683, 1999.
593 Atlas, D., Srivastava, R., and Sekhon, R. S.: Doppler radar characteristics of precipitation at
594 vertical incidence, Reviews of Geophysics, 11, 1-35, 1973.
595 Atlas, D., Ulbrich, C. W., Marks, F. D., Amitai, E., and Williams, C. R.: Systematic variation
596 of drop size and radar-rainfall relations, Journal of Geophysical Research: Atmospheres (1984–
597 2012), 104, 6155-6169, 1999.
598 Beard, K. V., and Chuang, C.: A new model for the equilibrium shape of raindrops, Journal of
599 the Atmospheric sciences, 44, 1509-1524, 1987.
600 Brandes, E. A., Zhang, G., and Vivekanandan, J.: Experiments in rainfall estimation with a
601 polarimetric radar in a subtropical environment, Journal of Applied Meteorology, 41, 674-685,
602 2002.
603 Bringi, V., Chandrasekar, V., Hubbert, J., Gorgucci, E., Randeu, W., and Schoenhuber, M.:
604 Raindrop size distribution in different climatic regimes from disdrometer and dual-polarized
605 radar analysis, Journal of the atmospheric sciences, 60, 354-365, 2003.
606 Chang, W.-Y., Wang, T.-C. C., and Lin, P.-L.: Characteristics of the raindrop size distribution
607 and drop shape relation in Typhoon systems in the western Pacific from the 2D video
608 disdrometer and NCU C-band polarimetric radar, Journal of Atmospheric and Oceanic
609 Technology, 26, 1973-1993, 2009.

610 Dou, X., Testud, J., Amayenc, P., and Black, R.: The parameterization of rain for a weather
611 radar, Comptes Rendus de l'Académie des Sciences-Series IIA-Earth and Planetary Science,
612 328, 577-582, 1999.
613 Feingold, G., and Levin, Z.: The lognormal fit to raindrop spectra from frontal convective
614 clouds in Israel, Journal of Climate and Applied Meteorology, 25, 1346-1363, 1986.
615 Göke, S., Ochs III, H. T., and Rauber, R. M.: Radar analysis of precipitation initiation in
616 maritime versus continental clouds near the Florida coast: Inferences concerning the role of
617 CCN and giant nuclei, Journal of the Atmospheric Sciences, 64, 3695-3707, 2007.
618 Gamache, J. F., and Houze Jr, R. A.: Mesoscale air motions associated with a tropical squall
619 line, Monthly Weather Review, 110, 118-135, 1982.
620 Gunn, R., and Kinzer, G. D.: The terminal velocity of fall for water droplets in stagnant air,
621 Journal of Meteorology, 6, 243-248, 1949.
622 Hu, Z., and Srivastava, R.: Evolution of raindrop size distribution by coalescence, breakup, and
623 evaporation: Theory and observations, Journal of the atmospheric sciences, 52, 1761-1783,
624 1995.
625 Johnson, R. H., and Hamilton, P. J.: The relationship of surface pressure features to the
626 precipitation and airflow structure of an intense midlatitude squall line, Monthly Weather
627 Review, 116, 1444-1473, 1988.
628 Kozu, T., Reddy, K. K., Mori, S., Thurai, M., Ong, J. T., Rao, D. N., and Shimomai, T.: Seasonal
629 and diurnal variations of raindrop size distribution in Asian monsoon region, JOURNAL-
630 METEOROLOGICAL SOCIETY OF JAPAN SERIES 2, 84, 195, 2006.
631 Leinonen, J., Moisseev, D., Leskinen, M., and Petersen, W. A.: A climatology of disdrometer
632 measurements of rainfall in Finland over five years with implications for global radar
633 observations, Journal of Applied Meteorology and Climatology, 51, 392-404, 2012.

634 Levin, Z.: Charge separation by splashing of naturally falling raindrops, Journal of the
635 Atmospheric Sciences, 28, 543-548, 1971.
636 Mapes, B. E., and Houze Jr, R. A.: Cloud clusters and superclusters over the oceanic warm
637 pool, Monthly Weather Review, 121, 1398-1416, 1993.
638 Markowitz, A. H.: Raindrop size distribution expressions, Journal of Applied Meteorology, 15,
639 1029-1031, 1976.
640 Marshall, J. S., and Palmer, W. M. K.: The distribution of raindrops with size, Journal of
641 meteorology, 5, 165-166, 1948.
642 Mueller, E. A.: Radar cross sections from drop size spectra, University of Illinois at Urbana-
643 Champaign, 1966.
644 Pruppacher, H., and Beard, K.: A wind tunnel investigation of the internal circulation and shape
645 of water drops falling at terminal velocity in air, Quarterly Journal of the Royal Meteorological
646 Society, 96, 247-256, 1970.
647 Qian, J.-H.: Why precipitation is mostly concentrated over islands in the Maritime Continent,
648 Journal of the Atmospheric Sciences, 65, 1428-1441, 2008.
649 Ray, P. S.: Broadband complex refractive indices of ice and water, Applied Optics, 11, 1836-
650 1844, 1972.
651 Sauvageot, H., and Lacaux, J.-P.: The shape of averaged drop size distributions, Journal of the
652 Atmospheric Sciences, 52, 1070-1083, 1995.
653 Seliga, T., and Bringi, V.: Potential use of radar differential reflectivity measurements at
654 orthogonal polarizations for measuring precipitation, Journal of Applied Meteorology, 15, 69-
655 76, 1976.
656 Sheppard, B. E.: Measurement of raindrop size distributions using a small Doppler radar. J.
657 Atmos. Oceanic Technol., 7, 255–268, 1990.

Sheppard, B. E. and P. I. Joe: Comparison of raindrop size distribution measurements by a Joss–Waldvogel disdrometer, a PMS 2DG spectrometer and a POSS Doppler radar. J. Atmos. Oceanic Technol., 11, 874–887, 1994.

Sheppard, B., and Joe, P.: Performance of the precipitation occurrence sensor system as a precipitation gauge, Journal of atmospheric and Oceanic technology, 25, 196-212, 2008.

Steiner, M., Houze Jr, R. A., and Yuter, S. E.: Climatological characterization of three-dimensional storm structure from operational radar and rain gauge data, Journal of Applied Meteorology, 34, 1978-2007, 1995.

Testud, J., Oury, S., Black, R. A., Amayenc, P., and Dou, X.: The concept of "normalized" distribution to describe raindrop spectra: A tool for cloud physics and cloud remote sensing, Journal of Applied Meteorology, 40, 1118-1140, 2001.

Tokay, A., and Short, D. A.: Evidence from tropical raindrop spectra of the origin of rain from stratiform versus convective clouds, Journal of applied meteorology, 35, 355-371, 1996.

Ulbrich, C. W.: Natural variations in the analytical form of the raindrop size distribution, Journal of Climate and Applied Meteorology, 22, 1764-1775, 1983.

Ulbrich, C. W., and Atlas, D.: Rainfall microphysics and radar properties: Analysis methods for drop size spectra, Journal of Applied Meteorology, 37, 912-923, 1998.

~~Waldvogel, A.: The N 0 jump of raindrop spectra, Journal of the Atmospheric Sciences, 31, 1067-1078, 1974.~~Waterman, P.C.: Matrix formulation of electromagnetic scattering. Proc. IEEE, 53, 805-812, 1965.

Waterman, P.C.: Symmetry, unitarity, and geometry in electromagnetic scattering, Physical review D, 3, 825, 1971.

Willis, P. T.: Functional fits to some observed drop size distributions and parameterization of rain, Journal of the Atmospheric Sciences, 41, 1648-1661, 1984.

You, C.-H., Lee, D.-I., and Kang, M.-Y.: Rainfall estimation using specific differential phase for the first operational polarimetric radar in Korea, Advances in Meteorology, 2014, 2014.

~~Zhang, G., Vivekanandan, J., and Brandes, E.: A method for estimating rain rate and drop size distribution from polarimetric radar measurements, Geoscience and Remote Sensing, IEEE Transactions on, 39, 830-841, 2001.~~

Tables

Tables 1. Specification of POSS disdrometer.

Specifications	Detail
Manufacturer	ANDREW CANADA INC
Module	PROCESSOR
Model number	POSS-F01
Nominal power	100 mW
Bandwidth	Single frequency
Emission	43 mW
Pointing direction	20 ° (to the vertical side)
Antenna	Rectangular pyramidal horns
Range of sample area	< 2 m
Wavelength	10.525 GHz ± 15 GHz
Physical dimension	277×200×200 cm^3
Net weights	Approximately 110 kg

Table 2. Designated date with respect to the source of rainfall.

Rainfall Category	Period			
	2001	**2002**	**2003**	**2004**
Typhoon	-	7.5-7.6, 8.31	5.29, 6.19, 8.7, 9.11-12	6.20, 8.19, 9.6
~~Chanma~~Changma	6.18-6.19, 6.23-6.26, 6.29-6.30, 7.1, 7.5-7.6 7.11-7.14	6.23-6.25, 6.30, 7.1-7.2	6.12-6.14, 6.23, 6.27 6.30, 7.1, 7.3-7.15	7.11-7.13, 7.14
Heavy rainfall	02.04.15. 20:13 to 02.04.16 06:29			
Seasonal	**Spring**	**Summer**	**Autumn**	**Winter**
	Mar. to May	Jun. to Aug.	Sep. to Nov.	Dec. to Feb.
Diurnal	**DT (KST)**		**NT (KST)**	
	0733 - 1712		1942 - 0509	

725

726

727

728 **Table 3.** Rainfall rate for each rainfall category and the number of sample size for 1-min data.

Rainfall Category	Total precipitation	Stratiform precipitation (%)	Convective precipitation (%)
Typhoon	5095	3118 (61.19)	652 (12.79)
Changma	18526	11099 (59.91)	1611 (8.69)
Heavy rainfall	359	153 (42.61)	150 (41.78)
Spring	30703	20370 (66.34)	1478 (4.81)
Summer	37187	22566 (60.68)	3409 (9.16)
Autumn	19809	12033 (60.74)	850 (4.29)
Winter	11689	7582 (64.86)	339 (2.90)
Daytime	41328	26373 (63.81)	2539 (6.14)
Nighttime	37455	23063 (84.00)	2242 (5.89)
Entire	99388	62551 (62.93)	6076 (6.11)

729

730

731

732

733 **Table 4.** DT and NT (KST) in Summer and Winter season.

Rainfall Category	Period	Beginning time (KST)	Finishing time (KST)
Summer	**DT**	0533	1927
	NT	1942	0509
Winter	**DT**	0733	1712
	NT	1819	0654

734

735

736

737

738

739

740

741

742

743

744

745

746

747

748 **Table 5.** Sum of the normalized wind direction frequencies between Summer and Winter.

Sum of the normalized wind direction frequencies				
Season	**Summer**		**Winter**	
Type	**Sea wind**	**Land wind**	**Sea wind**	**Land wind**
Frequency	0.4139	0.5861	0.3137	0.6863
Difference of the normalized wind direction frequency between DT and NT (DT-NT)				
Season	**Summer**		**Winter**	
Type	**Sea wind**	**Land wind**	**Sea wind**	**Land wind**
Frequency	0.0731	-0.0731	-0.0697	0.0697

749

750

751

752

753

754

755

756

757

758

759

760

761

762 **Figures**

763

764

765 **Figure 1.**

766 Photograph of the POSS instrument used in this research.

767

768

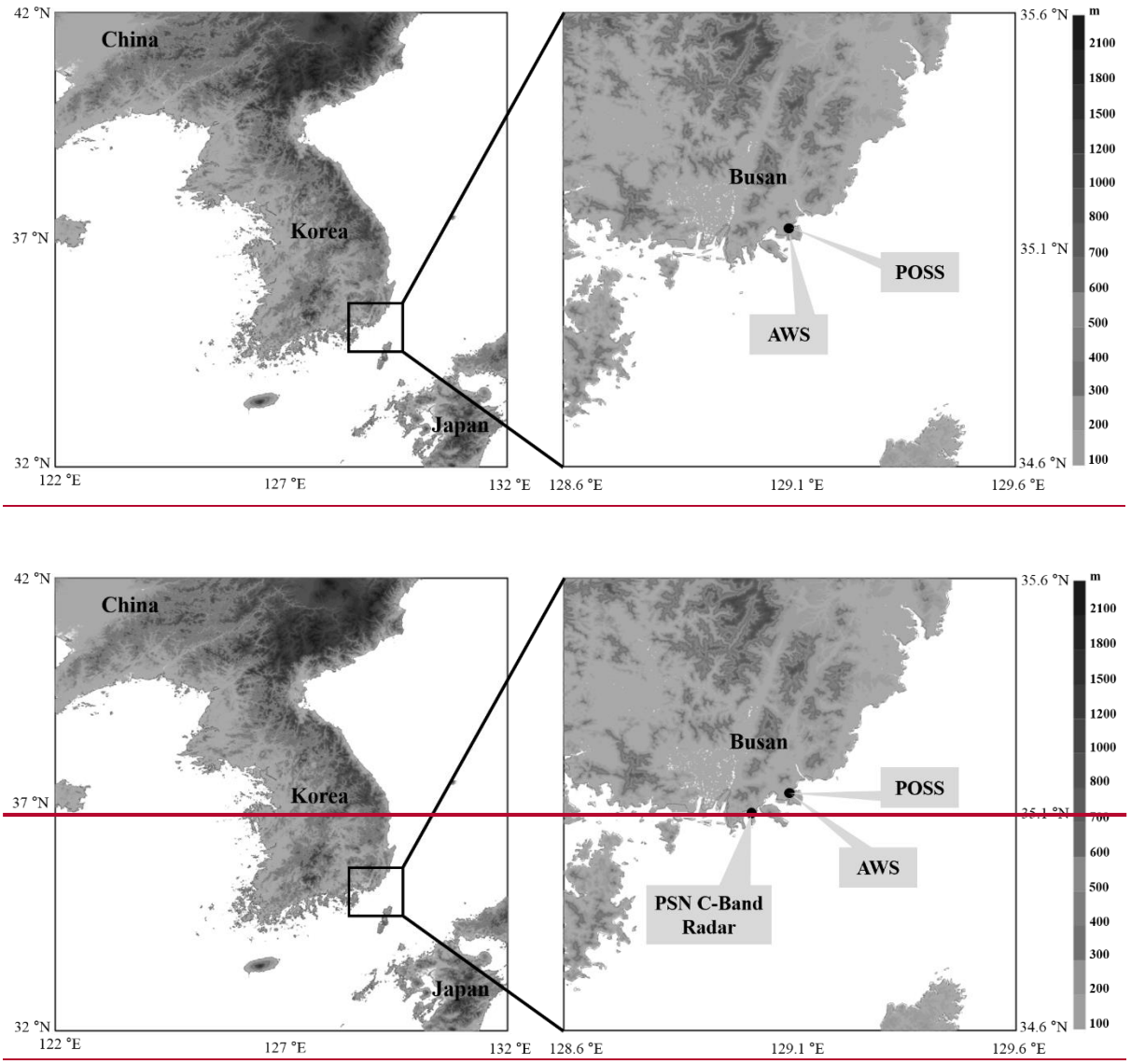

Figure 2.

Locations of the POSS and the AWS rain gauge installed in Busan, Korea.

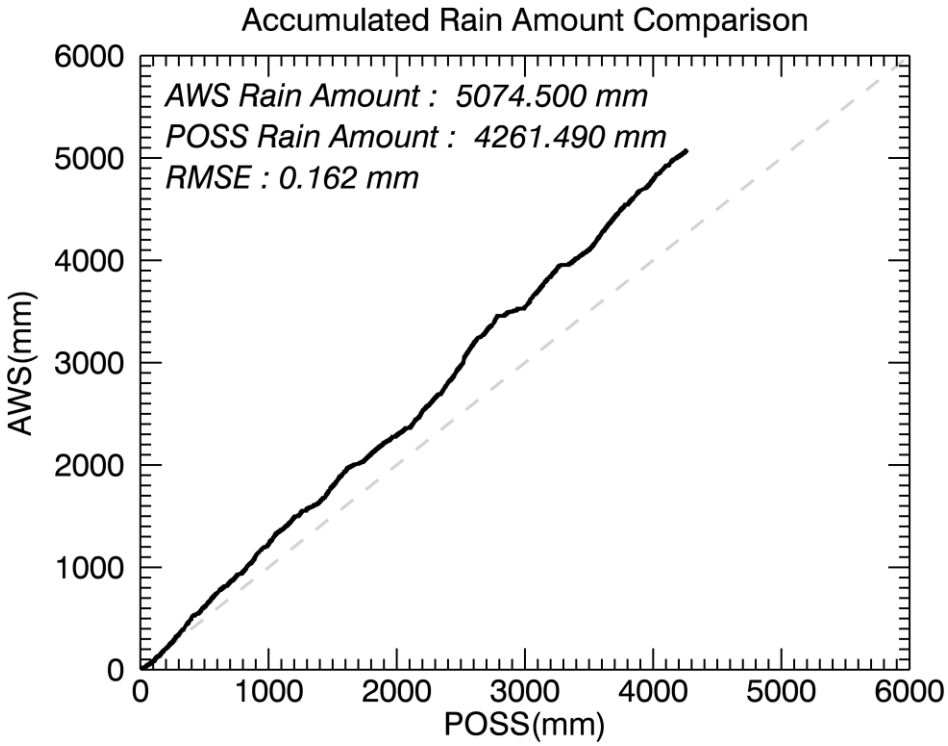

Figure 3.

Comparison of the recorded rainfall amounts between the POSS and AWS instrument.

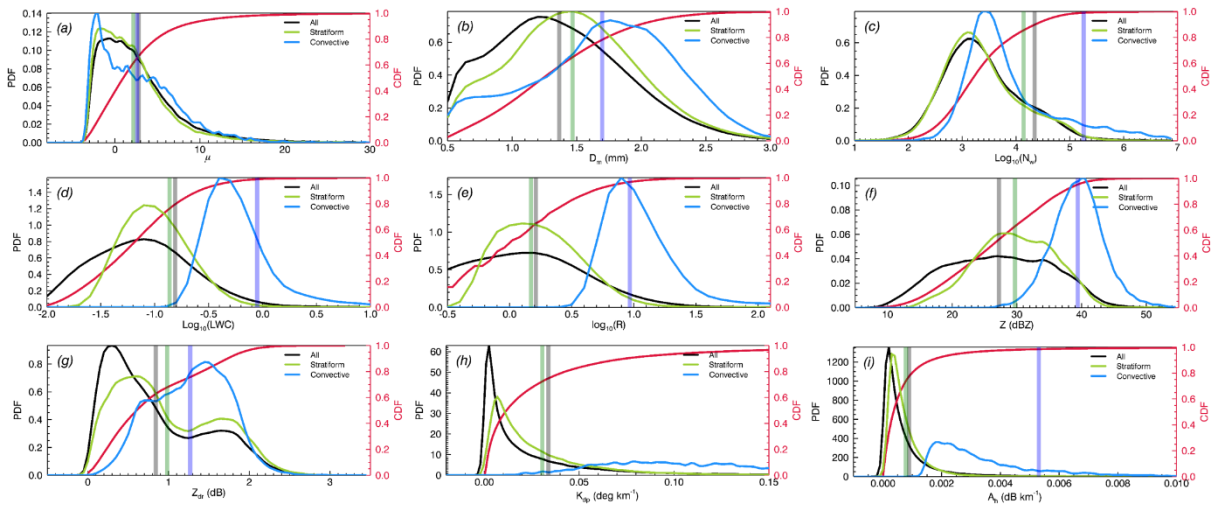

Figure 4.

PDF and CDF curves for (a) μ, (b) D_m, (c) $\log_{10}(N_w)$, (d) $\log_{10}(R)$, (e) $\log_{10}(LWC)$, (f) Z, (g) Z_{dr}, (h) K_{dp}, and (i) A_h for the entire rainfall dataset (solid black line), stratiform rainfall (solid green line), and convective rainfall (solid blue line). The solid red line represents the CDF for entire rainfall dataset. The solid vertical line represents the mean value of each type.

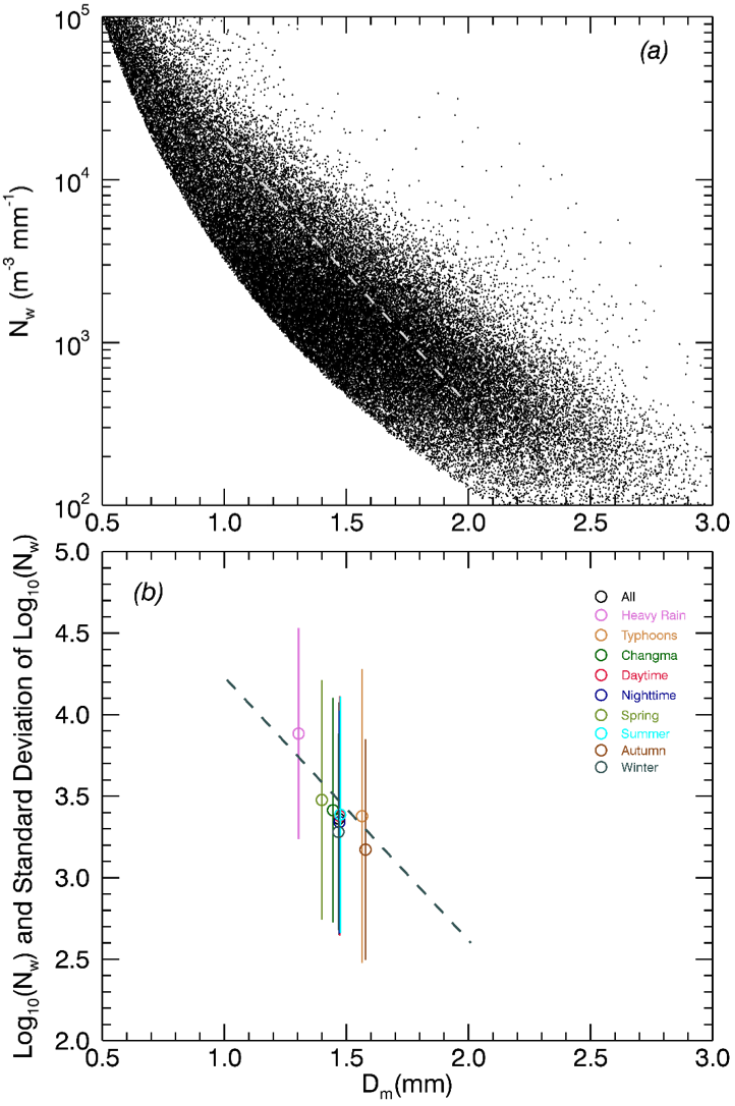

Figure 5.

(a) Scatter plot of 1-min D_m and N_w for the 10 rainfall categories with respect to stratiform rainfall data. The broken grey line represents the average line as defined by Bringi et al. (2003). (b) Scatter plot of mean D_m and $\log_{10}(N_w)$ values of the 10 rainfall categories with respect to stratiform rainfall and these mean values for each rainfall type are shown as circle symbols. The vertical line represents $\pm 1\sigma$ of $\log_{10}(N_w)$ for each category.

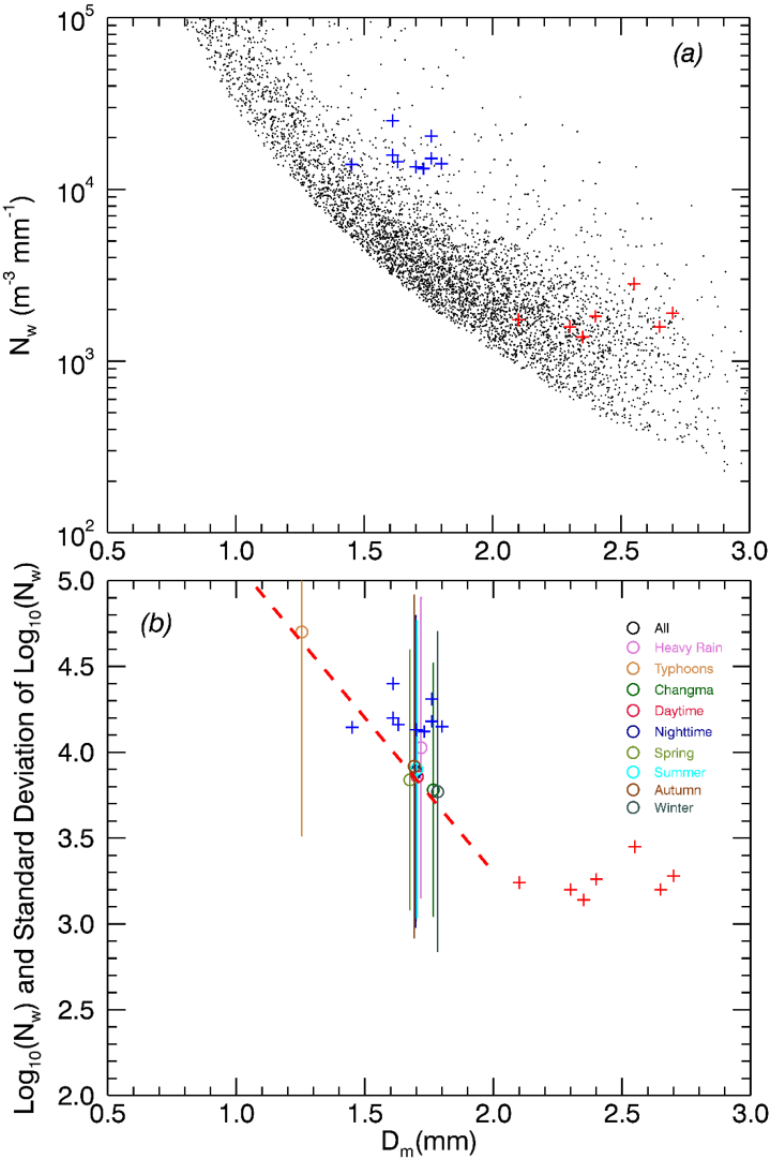

Figure 6.

(a) As in Figure 5(a), but for convective rainfall. The blue and red plus symbols represent maritime and continental rainfall, respectively, as defined by Bringi et al. (2003). (b) As in Figure 5(b), but for convective rainfall. The broken red line represents the mathematical expression described in Eq. (16).

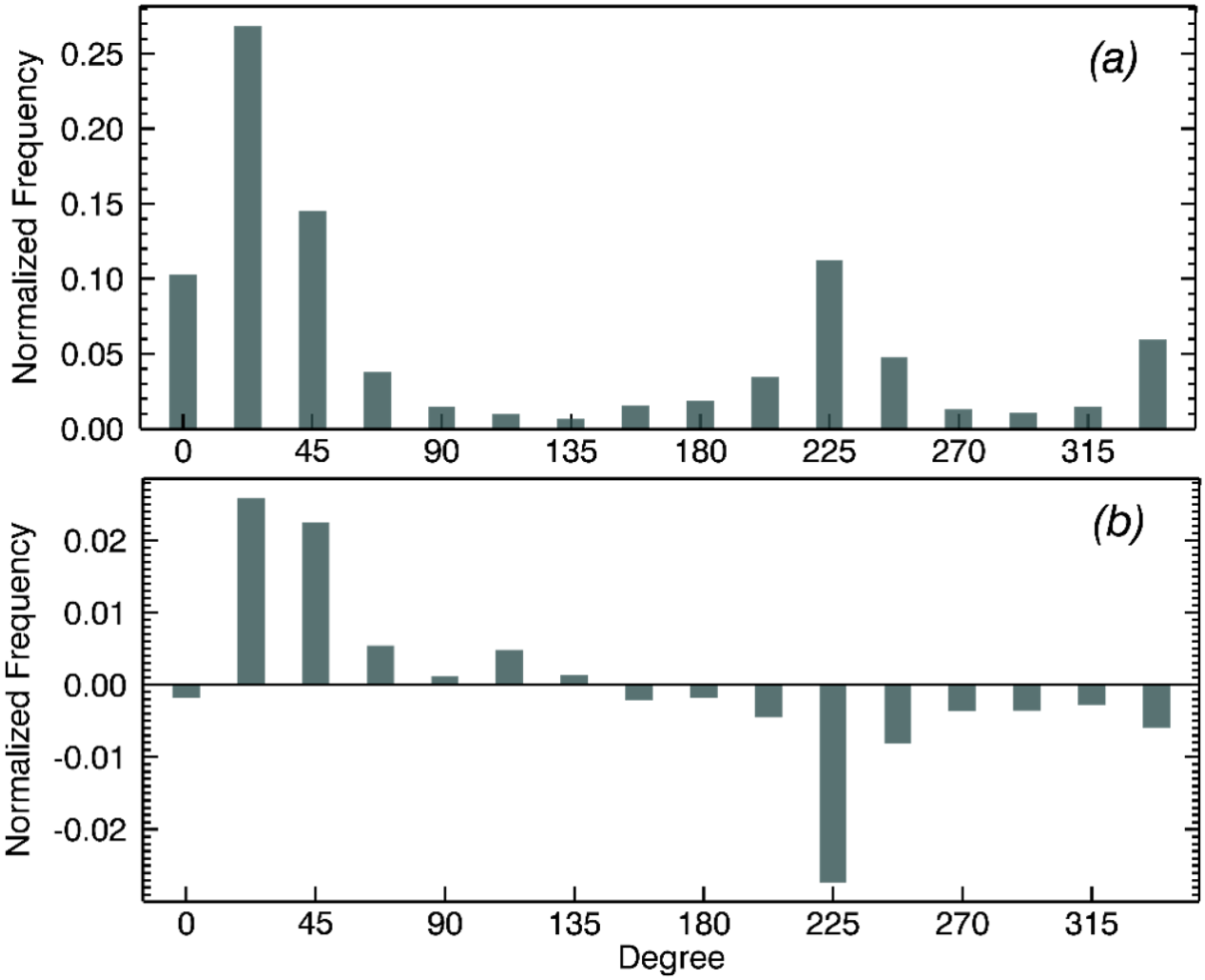

Figure 7.

(a) Histogram of normalized frequency of 16 wind directions for the entire study period. (b) Difference values of wind direction frequencies between DT and NT (DT - NT).

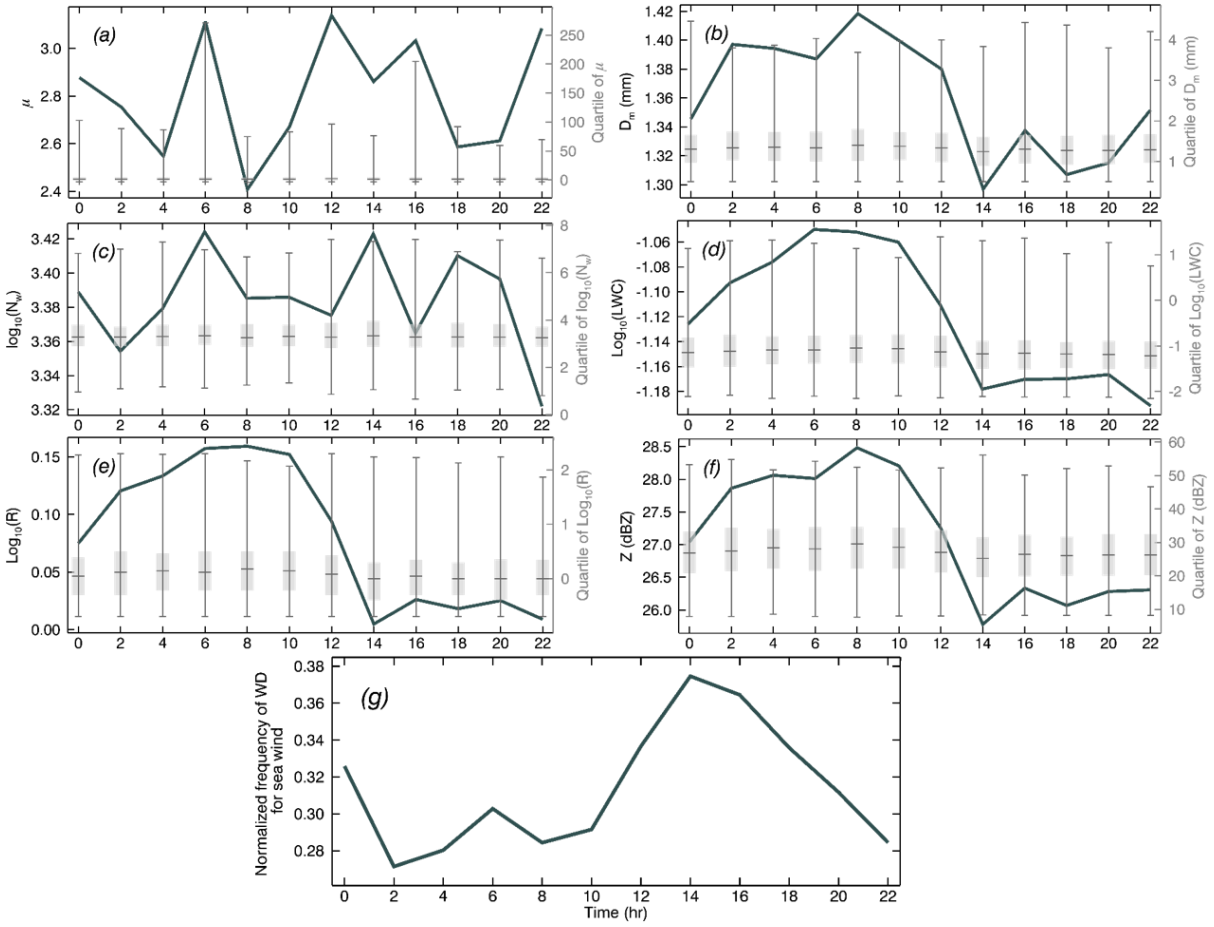

821

822 **Figure 8.**

823 Two hour interval time series of (a) μ, (b) D_m, (c) $\log_{10}(N_w)$, (d) $\log_{10}(R)$, (e)
824 $\log_{10}(LWC)$, (f) Z_h and (g) normalized frequency of wind direction for sea wind (45° to 225°)
825 with quartiles for the total period. Solid lines are quartiles for each time.

826

827

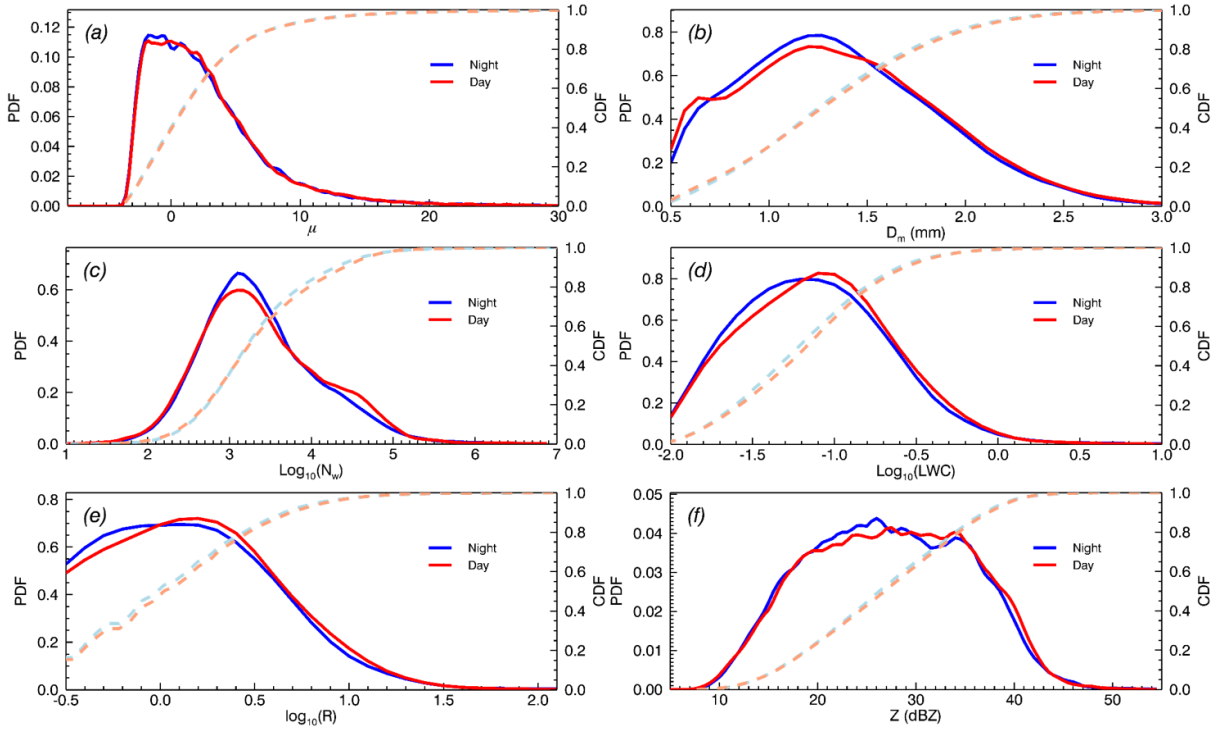

Figure 9.

PDF and CDF curves for (a) μ, (b) D_m, (c) $\log_{10}(N_w)$, (d) $\log_{10}(R)$, (e) $\log_{10}(LWC)$, and (f) Z for DT and NT according to the entire period. The solid red and blue lines represent the PDF for DT and NT, respectively. The broken light red and blue lines represent the CDF for DT and NT, respectively.

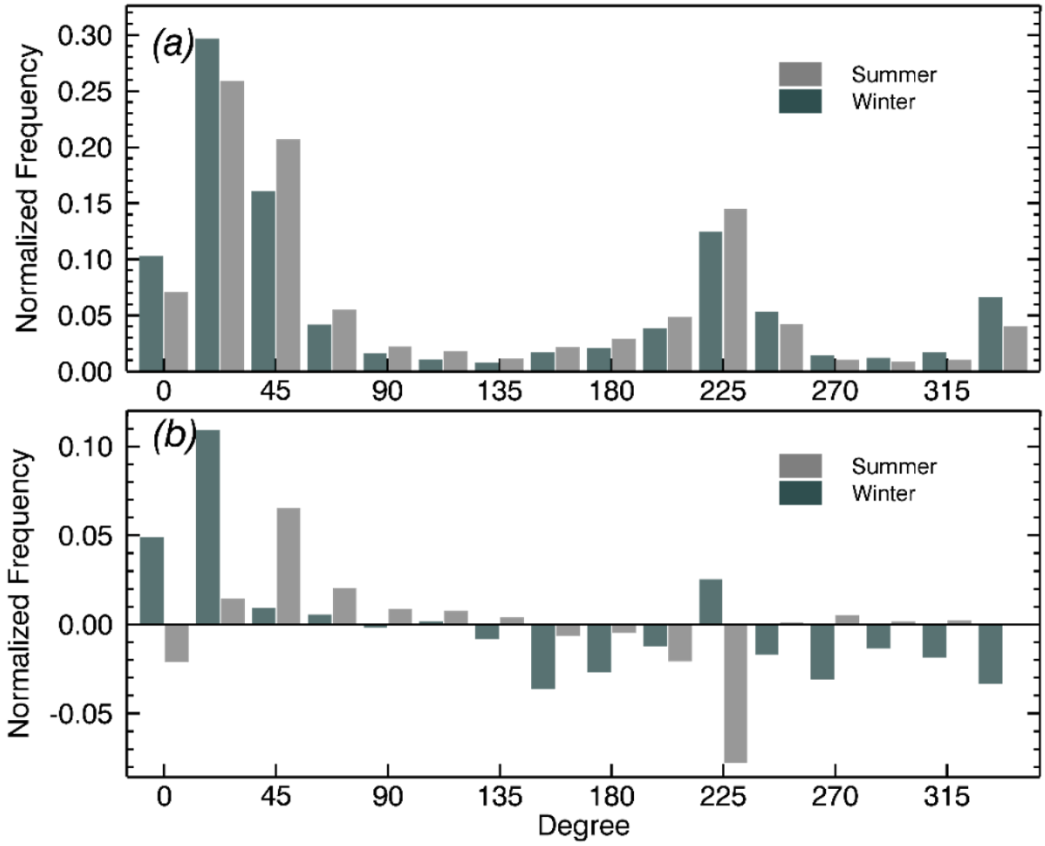

Figure 10.

Histogram of normalized frequency for 16 wind directions in (a) the entire period and (b) difference of normalized frequency of wind direction between DT and NT (DT – NT) for Summer (light grey) and Winter (dark grey) season.

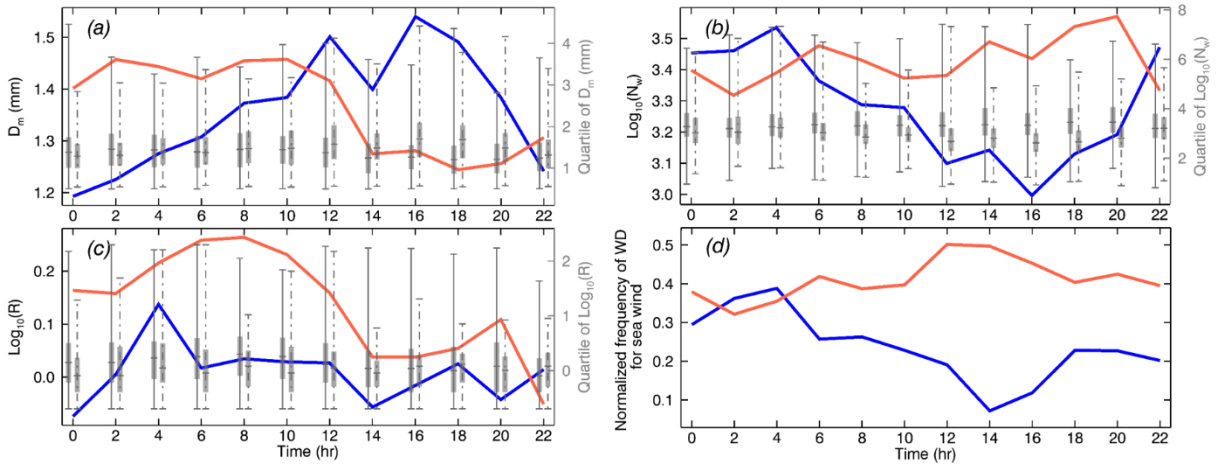

Figure 11.

Two hour interval time series and quartiles of (a) D_m, (b) $\log_{10}(N_w)$ (c) $\log_{10}(R)$ and (d) normalized frequency of wind direction for sea wind (45° to 225°) for the Summer (red) and Winter (blue) season. Solid (broken) lines are quartiles of Summer (Winter) for each time, respectively.

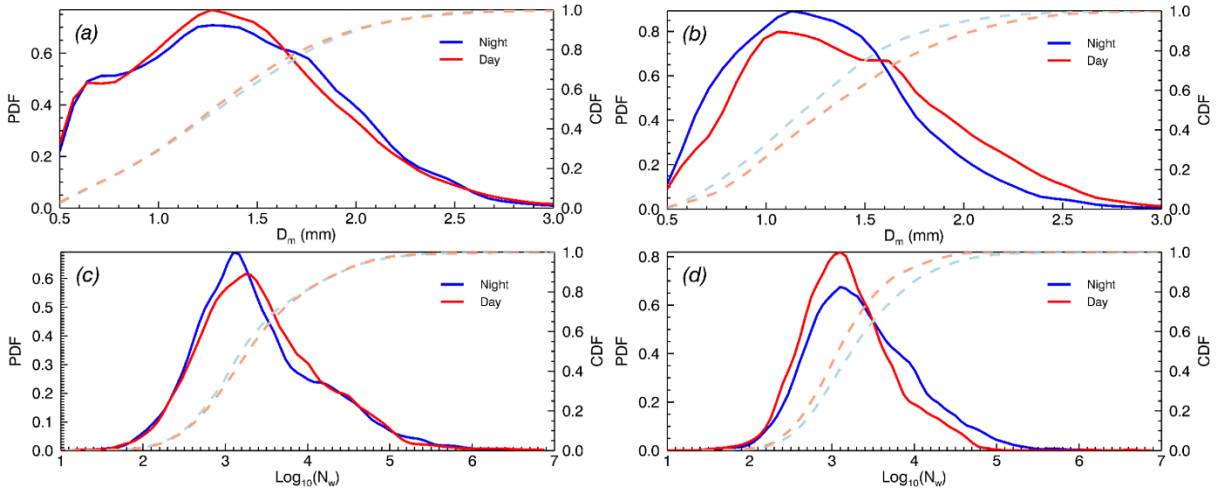

Figure 12.

PDF and CDF of (a) D_m ((b) D_m) and (c) N_w ((d) N_w) for the entire rainfall type in the Summer (Winter) season. Red and blue solid lines represent the PDF of DT and NT, respectively. The light red and blue broken line represent the CDF for each season

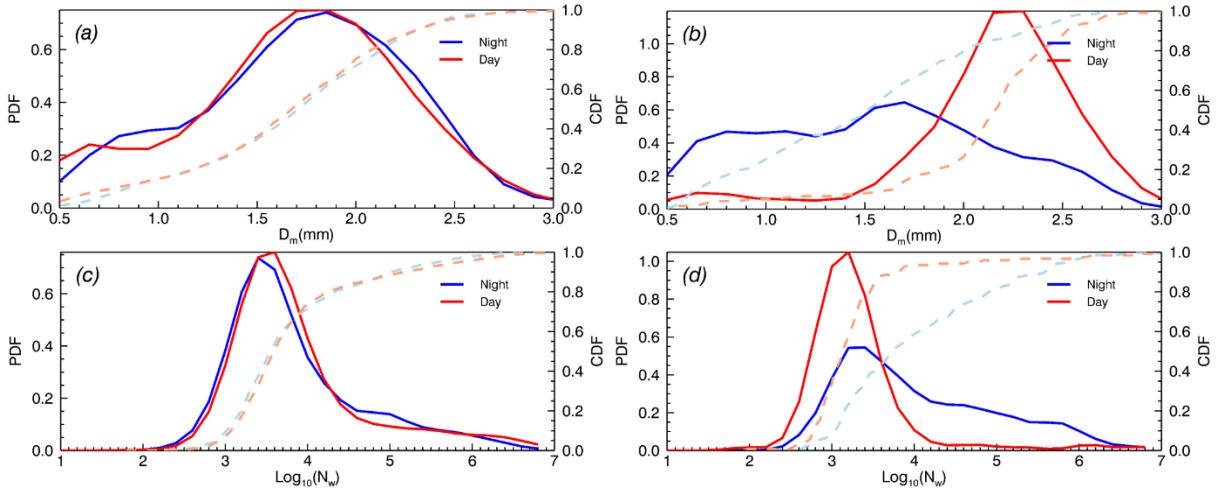

Figure 13.

As in Figure 12, but for convective rainfall type.